2011

Selection and enumeration of low EpCAM expressing breast cancer CTCs using a high throughput microfluidic device

Brandy Charon Snowden
Louisiana State University and Agricultural and Mechanical College, bsnowd1@lsu.edu

SELECTION AND ENUMERATION OF LOW EPCAM EXPRESSING BREAST CANCER CTCS USING A HIGH THROUGHPUT MICROFLUIDIC DEVICE

A Thesis

Submitted to the Graduate Faculty of the
Louisiana State University and
Agricultural and Mechanical College
in partial fulfillment of the
requirements for the degree of
Master of Science

in

The Department of Chemistry

by
Brandy C. Snowden
B.S. Southern University Agricultural and Mechanical College, 2007
December 2011

DEDICATION

This thesis is dedicated to my supportive and loving parents, Robert and Anna Snowden and my younger brother, Robert Snowden, Jr. Without their words of encouragement and prayers during some of the trying times of graduate school, I would have never made it through. For this, I will be forever grateful.

ACKNOWLEDGEMENTS

I would like to begin by acknowledging my advisor, Dr. Steven A. Soper for his patience and expertise that he offered to me throughout my thesis research. Dr. Soper's willingness to offer detailed critiques as well as share his seemingly endless wealth of scientific knowledge has made me the scientist that I am today. I also would like to acknowledge my committee members Prof. Kermit Murray and Prof. George Stanley for their cooperation as well as the insightful lectures that I experienced while at LSU.

I am also very grateful to Dr. Udara Dharmasiri for his presence when I was first introduced to circulating tumor cells project. I learned so much under his tutelage. I also would like to thank Dr. Samuel Ngorge for all of the insightful discussions that he provided when I reached points of confusion in my research. A special thanks is also in order for Swathi Pullagurla and Balamurugan Subramanian for their help in obtaining AFM images.

I am also grateful to have worked with other scientists in the Soper research group. These members include Dr. Hong, Dr. Chantiwas, Dr. Nesterova, Jerry, Edith, Mike, Joyce, Katrina, Brandon, Franklin, Kumuditha, Nyote, and Sudha. They were always willing to lend a hand whether it was for presentation practices or technical questions.

Finally, I would like to thank the Bridge to Doctorate Program for providing my funding the first two years of my graduate career.

TABLE OF CONTENTS

LIST OF TABLES

LIST OF FIGURES

ABBREVIATIONS AND ACRONYMS

CTC - circulating tumor cells
MDA-231 - breast cancer cell line
MCF-7 - breast cancer cell line
CCD – charge coupled device
CD - cluster of differentiation
CD34+ - hematopoietic stem cells
CD45 - leukocyte-specific antibody
DAPI - 4‘,6-diamidino-2-phenylindole
Ko - encounter rate
P - probability
Δ - dimensionless Damköhler number
kin - intrinsic antigen-antibody reaction rate
a - encounter radius
ʌ - dimensionless encounter time
U - cell-translational velocity
D - cell diffusion coefficient
Dh - hydraulic diameter
FA - adhesion force
FS - shear force
fc - bond strength between a single antigen-antibody complex
Cs - contact area of the cell
rp - cell radius
h and h‘ - cell-separation distances from the surface upon binding
EDC - 1-ethyl,-3-(3-dimethylaminopropyl)carbodiimide
NHS - N-hydroxysuccinimide
fNRBC - fetal nucleated red blood cell
εM - permittivity of the suspending medium
EpCAM - epithelial cell adhesion molecules
FACS - fluorescence-activated cell sorting
FITC - fluorescein isothiocyanate
HEPES - (4-(2-hydroxyethyl)-1-piperazineethanesulfonic acid)
HB - herringbone
HER- human epidermal growth factor
PBS – phosphate buffered saline
PDMS - polydimethylsiloxane
PFS – progression-free survival
PMMA - poly(methylmethacrylate)
PSMA - prostate-specific membrane antigen
Pt - Platinum
RT-PCR - reverse transcription polymerase chain reaction
STCs - -solid tumor cells
SELEX - systematic evolution of ligands by exponential enrichment
SiNP – silicon nanopillar
TP – tumor progenitor
UV - ultra violet
WBC - white blood cell
BM - basement membrane
ECM - extracellular matrix

VEGF - endothelial growth factor STC - solid tumor cells
A - Adenine
C - Cytosine
G - Guanine
T - Thymine
MES-2-(4-morpholino) - ethane sulfonic acid
Re - Reynolds number
FGF - fibroblast growth factor
U - velocity
FP - forward primer
RP - reverse primer
SEM - scanning electron microscopy
LDR - ligase detection reaction
CRC - colorectal cancer
FDA - food and drug administration
gDNA - genomic deoxyribonucleic acid
CE - capillary electrophoresis
PKH67 - fluorescein derivative
SW620 - colon cancer cells
KD - dissociation constant
H - total flow
ΔP - pressure drop
EOF - Electroosmotic flow
z - zeta Potential
Q - net negative surface charge
ρ - charge density
Uh - hydrodynamic flow velocity
UEOF - velocity due to electroosmosis flow
FITC - fluorescene isothicyanate
HSCs - hematopoietic stem cells
ssDNA - single stranded deoxyribonucleic acid
HTMSU - high-throughput microsampling unit

ABSTRACT

Breast cancer cells overexpress EpCAM that can be used as a marker to select breast cancer CTCs from heterogeneous clinical samples, even when present in low abundance. This study used MDA-MB-231 cells which have a low expression level of EpCAM (1.7×10^3 binding sites per cell.[3]) Herein, we will report on the use of antiEpCAM antibodies immobilized onto the surface of a capture bed poised within a PMMA microchip that was fabricated into an HTMSU used for selection of breast cancer CTCs seeded into a buffer solution. The microchannel walls within the capture bed were UV modified for 5, 10, 15 and 20 min and covalently decorated with antiEpCAM antibodies of varying concentrations (0.25, 0.5, 1.0 and 2.0 μg/μL) using an EDC-NHS coupling reaction. The HTMSU capture bed consisted of 51 high-aspect ratio microchannels (35 μm width × 150 μm depth) that were replicated in PMMA, from a metal mold master. Cultured breast cancer CTCs were fluorescently stained using a fluorescent isothiocyanate staining kit. The microfluidic device was infused with the fluorescently stained breast cancer CTCs at a flow rate of 27.5 uL/min. The capture of the cells was observed and visually quantified using a Zeiss inverted optical microscope.

Percent recoveries of breast cancer CTCs were obtained using HTMSUs that were UV modified for 5, 10, 15 and 20 min. The optimal percent recovery was 81.6% after 10 min of UV modification. Varying concentrations (0.25, 0.5, 1.0 and 2.0 μg/μL) of antiEpCAM antibodies were used and percent recoveries as low as 71.4% and as high as 81.6% were achieved using 0.25 and 1 μg/μL of antiEpCAM antibody respectively.

Lastly, another method for decorating the microfluidic channels with antiEpCAM antibodies was explored. Using 2 min exposure to plasma oxidation, antiEpCAM antibodies were immobilized to the microchannel walls. Following the same cell selection protocol used for the UV modified HTMSU, a mean percent recovery of 50% was obtained. The combination of carboxylate, oxides and anhydride groups formed due to plasma oxidation, instead of exclusively carboxylate groups that form due to UV modification could be a contributing factor to this lower recovery.

CHAPTER 1. CIRCULATING TUMOR CELLS (CTCs)

1.1. Low Abundance Cells

The enumeration and analysis of low abundance cells is advantageous because of its various applications such as cancer research, forensic science, homeland security and environmental analysis. Low abundance cells are described as cells that are present at concentrations less than 1,000 cells/ volume of fluid. [1] Some typical examples of low abundance cells are circulating fetal cells, stem cells and circulating tumor cells (CTCs). A major challenge that affects the analysis of low abundance cells is the selection of target cells from a heterogeneous population in which the target is the minority. There are four important metrics that must be considered for the isolation of low-abundance cells: *(a)* Throughput, the number of cell identification or sorting steps per unit time; *(b)* recovery, an indicator of target cells collected from the input sample; *(c)* purity, which depends on the number of interfering cells excluded from the final analysis; and *(d)* viability, which describes whether or not the isolated cells retain their biological function after the selection process.[2, 3]

1.2 Significance of CTC Analysis

The challenge of selecting low abundance cells from a heterogeneous population is exemplified in the analysis of CTCs, especially those that have low expression levels of EpCAM.

CTCs are cells that are released from a primary tumor into circulation and carried to a secondary site, where they can spawn metastatic disease.[1] CTCs can be generally defined as nucleated cells that lack CD45 and express cytokeratin(s).[4, 5] Cytokeratin is an epithelial subgroup of a class of proteins termed intermediate filaments (IF). IF proteins are used in pathology for the classification of normal and malignant cells on a molecular basis. In recent years, many investigators have outlined a variety of applications of CK polypeptides as diagnostic markers in tumor pathology, particularly for the differential diagnosis of carcinomas at the histologic level.

An antibody to the membrane antigen epithelial cell adhesion molecule (EpCAM) is used to identify cells of epithelial origin circulating within the blood.[6] Additionally, cytokeratin antibodies can be used to further distinguish CTCs as those that are not white blood cells (i.e. - CD45 negative) and select for

carcinomas..[7]

CTCs were first discovered by the Austrian physician, Thomas Ashworth, in the autopsy of a patient who succumbed to advanced metastatic cancer and were reported in 1869.[8] In 1889, the seed and soil hypothesis for understanding the process of metastasis was proposed by Paget.[9] He hypothesized that metastatic spread was the result of particular tumor cells (seeds) finding a feasible environment (soil) in which to develop and grow. An alternative hypothesis of mechanical entrapment was proposed by Ewing.[11] In 1928, Ewing suggested that CTCs accumulate through entrapment in the first vascular bed they encounter.

Metastasis can be described as the process in which cancer cells leave the primary tumor site, disseminate and form secondary tumors at anatomically remote sites.[10] CTCs have also been observed in animals that were implanted with experimental tumors. The cells were seen to be released into the blood and it was also shown that trauma produces an increased release of CTCs and an increase in metastasis. It was calculated that $1x10^5$ cells were released per day in a highly metastatic tumor system.[11]

Based on these hypotheses, metastasis is often described as a cascade of events (Figure 1.1), because there are a series of steps that are involved: (1) Angiogenesis, which is the development of a new blood supply for the proliferating cells; (2) tumor cells eluding from the primary tumor mass; (3) migration and incursion of tumor cells through the basement membrane (BM) and extracellular matrix (ECM) surrounding the tumor epithelium and invasion of the BM supporting the endothelium of local blood vessels; (4) intravasation of the tumor cells into the blood vessel before traveling hematogeneous (lymphagenous) dissemination to distant anatomical sites; (5) CTC adhesion to the endothelial cell lining at the capillary bed of the target organ site; (6) tumor cells incursion through the endothelial cell layer and surrounding BM (extravasation) and target organ tissue; and (7) secondary tumor foci growth at the target organ site.[10, 11, 12]

The formation of new blood vessels from pre-existing vasculature is termed angiogenesis.[13] The formation of an intra-tumor blood supply gives tumors the ability to obtain the oxygen and nutrients necessary to flourish. The release of growth factors, such as vascular endothelial growth factor (VEGF)

and fibroblast growth factor (FGF) stimulate angiogenesis. Through angiogenesis, tumors are able to gain access to a blood supply in conjunction with co-option of existing blood vessels and also vasculogenic mimicry, which causes the tumor cells to carve blood vessel-like conduits. [14]

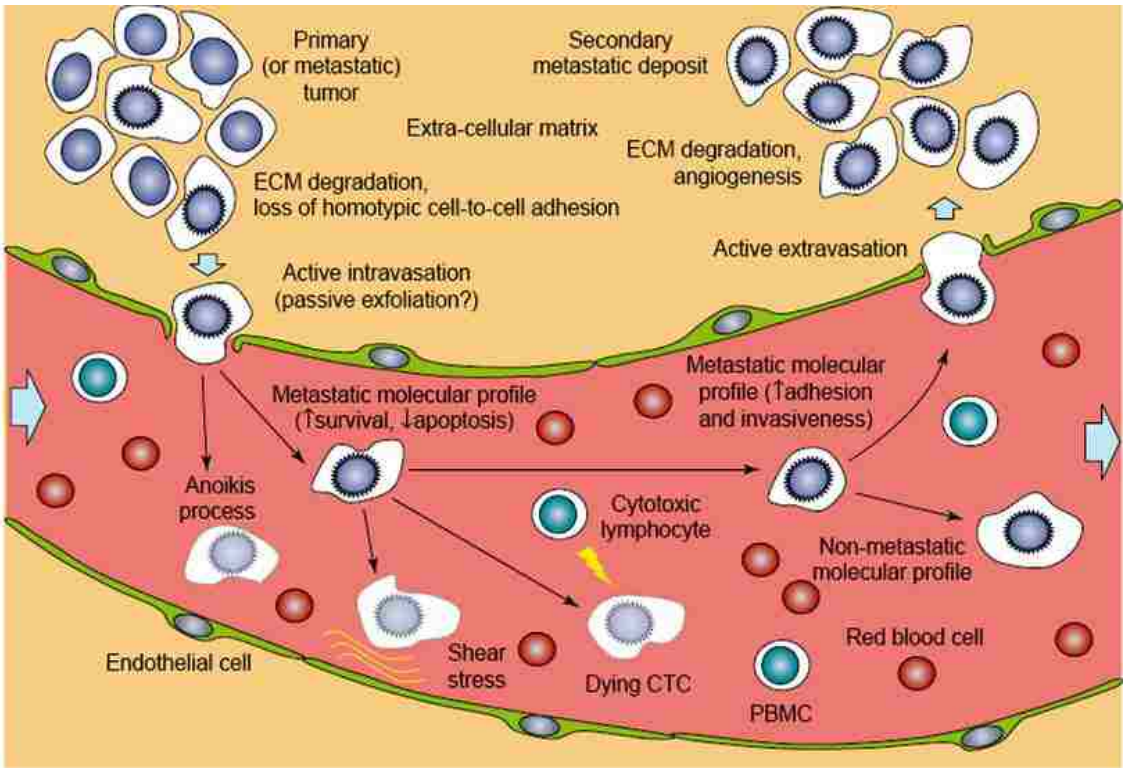

Figure 1.1 The metastatic cascade. Tumor cells are released from the primary tumor mass, and thus become circulating tumor cells (CTCs). The CTCs in the blood are subjected to the shear forces generated by the flow of blood, immune response attack and anoikis. CTCs that do survive can reach a target organ and attach to the endothelial cell lining within the capillary bed of the target site. After invading the endothelium, a secondary tumor mass can develop. Reprinted with permission.[11]

The initial phases of dissemination are promoted by the loss of cell-cell adhesion within the primary tumor mass, which permits disaggregation.[14] Cadherin/catenin expression in the primary tumor is also altered and results in the loss of cell–cell adhesion. Abrogration of E-cadherin has been reportedly associated with the metastatic phenotype.[15] Dissolution of the ECM during metastasis occurs through the action of several hydrolytic enzymes, released either by the tumor cells themselves or by cells surrounding the tumor cells.[16]

Following their release from the primary tumor site, many cancer cells possess the ability to migrate

in several different ways: (1) Moving together as groups or as single cells; (2) assuming an elongated mesenchymal morphology; or (3) crawling in an amoeboid fashion. Initially, tumor cells attach to the BM and ECM through interactions with the integrin family of adhesion receptors and subsequently traverse these structures as proteolytic enzymes aiding their invasion and ultimately allowing the tumor cells access to the vasculature.[12] Tumor cells also can physically deform their shape in order to move through collagenous matrices. [17]

Detached tumor cells are allowed to pass into systemic circulation, because of endothelial cells' ability to retract. CTCs in the blood stream are subject to events in the blood stream that threaten their survival including the shear forces generated by the flow of blood and an immune response attack.[17] Once the CTCs are shed, they are fragile and lack interactions with blood borne fibrin and platelets and consequently, the membrane can be easily destroyed by shear stress imparted by blood flow.[17]

1.3 Evidence for Breast Cancer CTC in Early Metastasis

The majority of current understanding of the processes involved in cancer metastasis has been originated from mouse models of metastasis.[18] Originally, it was believed that metastasis is an event that occurred late in cancer progression, but evidence gathered from CTCs has shown that metastasis may be an early event.[19] This is also supported by the fact that CTCs have been discovered in patients with early breast cancer.[19]

A study recently conducted by Husemann *et al*. utilizing transgenic (HER2/PyMT) mice showed that dissemination of tumor cells can occur at the pre-invasive stage of the primary tumor.[20] Cancer cells that are transported through the circulation from the primary tumor to vital organs throughout the body, initiate blood-borne metastasis. This mechanism is directly responsible for the majority of cancer related deaths.[18]

Tumor cells that express invasive phenotypes lose many types of epithelial antigens in a transformation process called epithelial-mesenchymal transition (EMT).[21] The loss of epithelial antigens occurs when non-motile epithelial cells with regular cell-cell junctions and adhesion, lose their cell-cell junctions and convert into individual, motile and invasive mesenchymal phenotypic cells.[21] These

processes are consistent with the acquisition of a "cancer stem-like cell" phenotype that is also known as "stemness" or cancer stem cell (CSCs) characteristics.[21] The EMT is a dynamic and reversible process, which has been observed in patient tissues to display a wide spectrum of phenotypes.[22] EMT occurs early in cancer progression and involves tumor progenitor (TP) cells with stem/invasive cell properties. These types of cells may enter the circulation to generate multiple populations of CTCs with specific phenotypes that could contribute to aggressive growth of tumor cells and to early metastatic colony formation.[23] EMT is known to induce tumor cell motility, aggressiveness and invasiveness, therefore promoting metastasis of solid carcinomas.[24]

1.4 Breast Cancer CTCs

CTCs have been detected in the majority of epithelial cancers, such as prostate, lung, colon and breast, which is the focus of this thesis.[25] The prognoses for women with metastatic breast cancer (MBC) represent a heterogeneous group and can vary depending on factors such as age, tumor hormone-receptor status and grade, anatomic site, and extent of disease, as well as the status of any conditions and associated performance status. Breast cancer is one of the most common cancers that afflict women. The American Cancer Society reports that in 2010, approximately 207,090 new cases of invasive breast cancer were diagnosed and of those, 39,840 women died from metastatic disease. These statistics make the need for novel approaches for breast cancer diagnosis more urgent.[19]

CTCs in breast cancer patients have been shown to be an indicator of poor prognosis when the CTC level in circulation exceeds a particular level. The presence of high CTC counts (≥5 per 7.5 mL of whole blood) is associated with shorter progression-free (PFS) and overall survival (OS) in the metastatic setting.[26] Progression free survival describes the length of time during and after treatment that the disease being treated does not get worse. Overall survival differs from PFS in that it involves the percentage of cancer patients in a group that will stay alive after a certain period of time.[22] The prognostic value of CTCs is unrelated to hormonal receptor status, sites of recurrence, and previous treatments, and has been demonstrated superior to tumor burden, suggesting a further peculiar biological value.[26]

1.5 Utility of CTCs in a Clinical Setting

Increasingly advanced and sensitive technologies to isolate human CTCs have emerged and provide the opportunity to extend studies of cancer metastasis directly to human cancer.[18] Potential applications for CTC analyses include real time noninvasive monitoring of CTCs as biomarkers of either sensitivity or acquired resistance to new cancer therapies and identifying new potential therapeutic targets to directly suppress cancer.[18]

There are challenges to be considered involving CTCs in the clinical setting. Studies have shown remarkably varying CTC numbers ranging from <5 to thousands per mL in the same category of patients.[26] These differences in CTC numbers could be caused by cancer biology or varying sensitivity of techniques used, but clarification of these possibilities is still necessary. Ultimately, the heterogeneity of breast cancer subtypes makes it difficult to rely on a single, universally expressed and specific marker.[26]

Despite these challenges, the enumeration of CTCs has been shown to offer information regarding patient prognosis and may be able to provide oncologists with information about patient response to systemic therapy shortly after its initialization.[26] Ideally, physicians would be able to determine a patient's sensitivity or resistance to planned treatment and identify indicators of good and poor prognosis. They will also be able to detect markers of resistance that may be forming during the treatment.[27]

There are two types of distinct marker types that are expressed on CTC membranes, tumor type-specific and epithelial-specific markers.[28] Tumor type-specific markers are expressed only by tumor cells that have disseminated from a particular tumor. Examples of this type of marker include mammoglobin, HER2-neu, mucin 1 (breast cancer), prostate specific antigen (prostate cancer), and carcinoembryonic antigen (colorectal and gastric cancers). [4, 29] These types of markers not only offer the potential advantages of specifically identifying a particular organ tumor cell rather than just epithelial cells but they also provide some insight into their molecular characteristics. [30]

The most frequently used CTC isolation techniques often rely on antibody-based capture of CTCs, which express epithelial cell surface markers that are not present in normal leukocytes.[4, 26] Of these epithelial cell surface markers, epithelial cell adhesion molecule (EpCAM) is most commonly used

because its expression is virtually universal in cells of epithelial origin, and it is also absent in blood cells.[18] In primary and metastatic breast cancers, EpCAM is expressed at levels that are 100- to 1,000 times greater than in benign epithelial cells, and is thought to be linked to tumor invasion and migration. The overexpression of EpCAM in carcinomas has been found to be associated with poor prognosis and therefore leads to the evaluation of EpCAM as a potential therapeutic target for patients with advanced carcinomas.[31]

1.6 CTC Morphology

In order to possess the capability to capture CTCs, technological platforms have been developed that exploit the observation that CTCs have a larger median diameter (15 μm) than normal cells (11 μm) [27] Solid tumor cells (STCs) have a slightly larger nuclear/cytoplasmic (N/C) ratio compared to CTCs (CTCs-27.1%, STCs-28.9%).[28] CTCs have a round or oval morphology while STCs and even cultured CTCs have irregularly-shaped nuclei. Many CTCs contain conspicuous intracellular compartments that contain multiple small vesicles and large amounts of amorphous material. A ribosome decorated membrane also surrounds these CTCs; these inclusions could have a size that is equal to or exceeds that of the nucleus and are not seen in STCs. [8]

1.7 Macroscale Method for CTC Analysis: Cell Search™

The first and only CTC isolation device to obtain FDA approval is the CellSearch™ system.

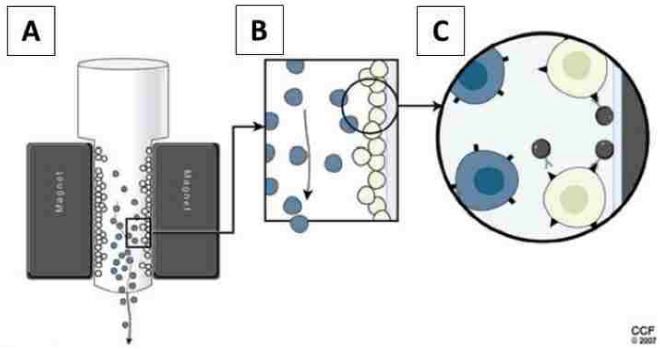

Figure 1.2 (A-C) Schematic of the immunomagnetic-assisted cell-sorting process. Blue and tan circles represent normal and circulating tumor cells, respectively. [33]

It is an immunomagnetic isolation system for selecting CTCs from peripheral blood samples using

positive selection (Figure 1.2) with EpCAM used as the antigenic marker.

This system uses magnetic beads that are conjugated to monoclonal antibodies directed against EpCAM. The processed sample is first enriched with ferromagnetic particles coated with anti-EpCAM antibodies for selecting the CTCs. Following this, density gradient centrifugation is utilized along with a series of washes, in order to remove the red blood cell (RBC) fraction from the sample. These immunomagnetically-labeled cells are then isolated by an external magnetic field. After magnetic isolation, the cells are incubated with phycoerythrin-conjugated anti-cytokeratin antibodies that specifically recognize cytokeratins to identify epithelial cells, an antibody against CD45 conjugated with allophycocyanin to identify contaminating leukocytes, a nuclear dye [4**,** 6-diamidino-2-phenylindole (DAPI)] to fluorescently label the cell nucleus, and a permeabilization buffer to allow cytokeratin antibodies to enter into the CTCs. [18, 31]

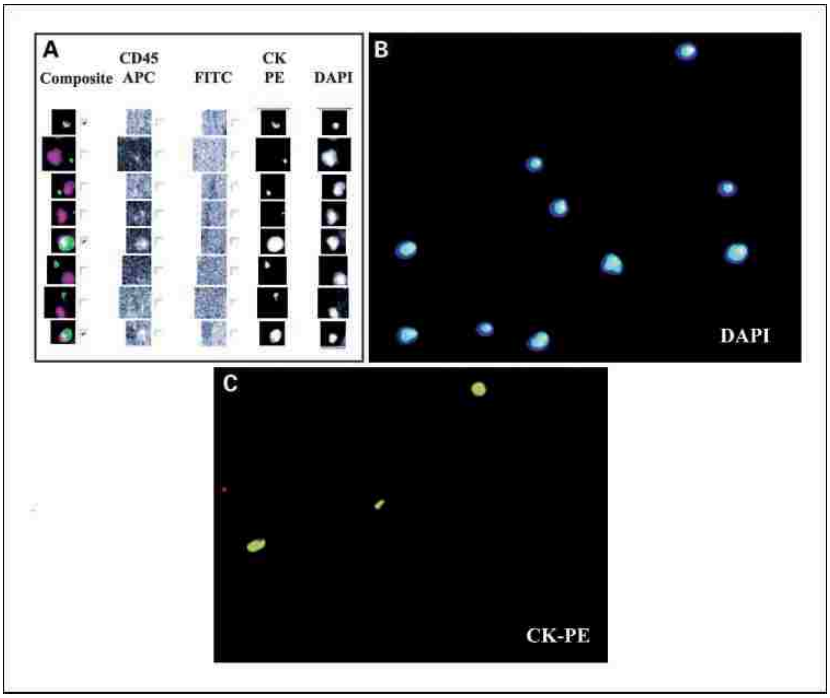

Figure 1.3 (A) Gallery of images that has been screened for CTCs. Three CTCs are marked in the composite image, which are positive for DAPI and cytokeratin-phycoerythrin (green) but negative for CD45-APC (allophycocyanin) and in the FITC (fluorescein) channel. (B) DAPI staining of nuclei and (C) cytokeratin-positive CTCs.[31]

The CellSearch system has a recovery of about 60%. Some of the limitations with this system include

its low throughput, modest recovery and purity and high input volume required.[31]

The theory that the presence of breast cancer CTCs effects overall survival rate was investigated by Cristofanilli et. al using CellSearch™ One hundred and seventy five patients with measured MBC were involved in the study, 83 of these were beginning first line treatment and were the focus of this study. A 7.5 mL of whole blood sample was drawn prior to treatment initiation and monthly for 6 months thereafter and were isolated and quantified using immonomagnetics.[30]

Figure 1.4 shows Kaplan-Meier plots for prediction of PFS and OS using baseline CTC numbers

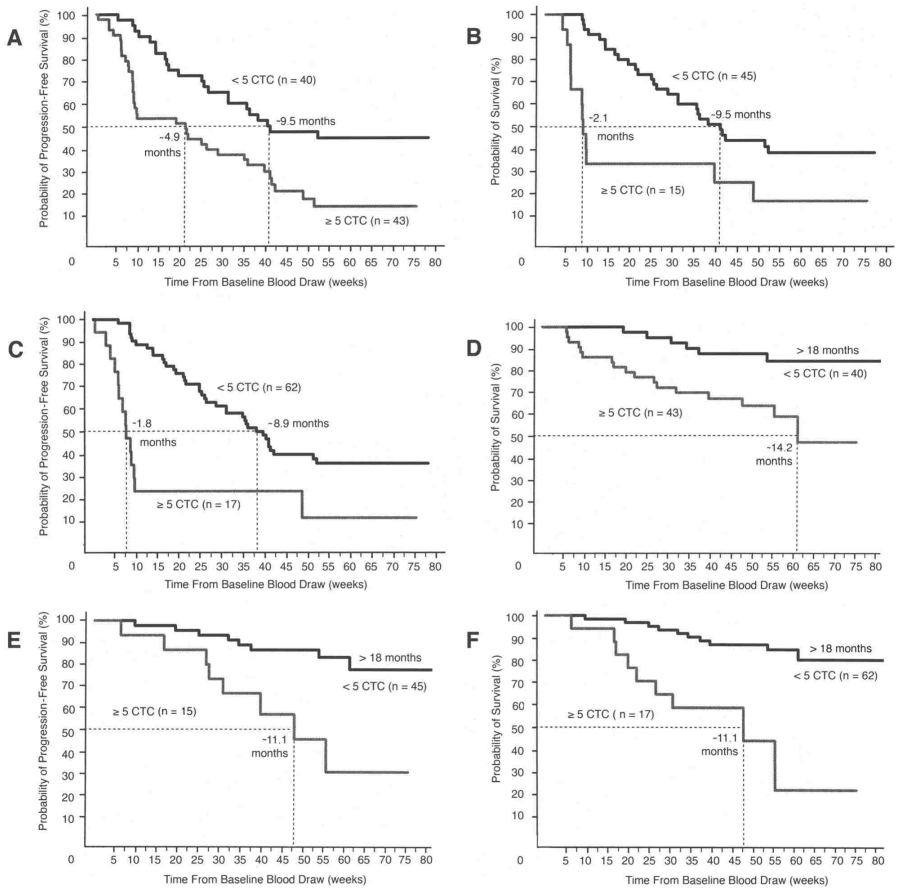

Figure 1.4. Kaplan-Meier plots of progression-free survival (PFS) and overall survival (OS) in first-line therapy MBC patients with less than five circulating tumor cells (CTCs; top lines) or five CTCs (bottom lines) at baseline (A and D), first follow-up visit (B and E), and restaging (C and F). PFS and OS were calculated from the time of the baseline blood draw. Coordinates of dashed lines indicate median survival time. [30]

(Figs 1.4A and D, n=83 patients), the first follow-up CTC numbers (Figs 1.4B and E, n=60 patients), and

the CTC numbers at restaging (Figs 1.4C and F, n =79 patients). Forty-three of the patients (52%) had ≥ 5 CTCs per 7.5 mL of blood at baseline. These patients had a notably shorter median PFS (~4.9 months; 95% CI, 2.0 to 8.1 months) and median OS (~14.2 months; 95%CI, 11.1 to >18 months) in comparison to patients with <5 CTCs per 7.5 mL of blood (median PFS, ~9.5 months; 95% CI, 6.1 to > 18 months; *P* = .0014; median OS >18 months; *P*<.0048). Baseline CTC number was almost always associated with PFS in patients whose initial therapy was chemotherapy. Cristofinilli concluded that the presence of 5 or more CTCs in 7.5 mL of blood at the time of diagnosis of metastatic breast cancer and preceding initiation of first line therapy is linked to short PFS and OS.[30]

1.8 Methods of CTC Analysis Using Microfluidics

There are several characteristics that a platform for capturing CTCs should possess, such as high sensitivity, meaning it has the ability to detect every single CTC. It should also demonstrate a high level of purity. Most importantly, this method should preserve the CTC viability and morphology.[24] Current methods for CTC isolation have attempted to exploit characteristics that are specific to CTCs.

There have been many recent technological advances for the detection and analysis of CTCs. Microfluidic devices provide important advantages over other purification techniques because they enable highly efficient processing of complex fluids while causing minimal damage to sensitive cell populations.[34] One such method for CTC analysis is the microfluidic device developed by Nagrath *et. al* termed the "CTC chip" (Figure 1.5 B).[35] This "first generation" device has the ability to efficiently and reproducibly isolate CTCs from the blood of patients with common epithelial tumors. The microfluidic system (Figure 1.5C) consisted of a microfluidic chip etched in silicon (Fig. 1.5B), a manifold that encloses the chip (Figure 1.5C), and a pneumatic pump (Figure 1.5A) that establishes the flow through the capture module (Figure 1.5C). The chip has dimensions of 25 mm × 66 mm, with an active capture area of 19 mm × 51 mm. It consisted of an equilateral triangular array of microposts, 100 μm tall and 100 μm in diameter with an average 50 μm gap between microposts. In order to increase the hydrodynamic efficiency, the repeated patterns of equilateral triangular arrays were shifted vertically by 50 μm for every three rows throughout the chip to ensure maximum interactions between micropost structures and cells.

This array incorporated 78,000 microposts within a surface area of 970 mm^2. The chip employed deep reactive ion etching (DRIE) for its fabrication.[33]

The two essential operating parameters for controlling the efficiency of cell capture are sample flow velocity and shear force. The flow velocity controls the length of time that the cell interacts with the micropost. The shear force must be kept low to ensure that the cells are adequately attached to the micropost.

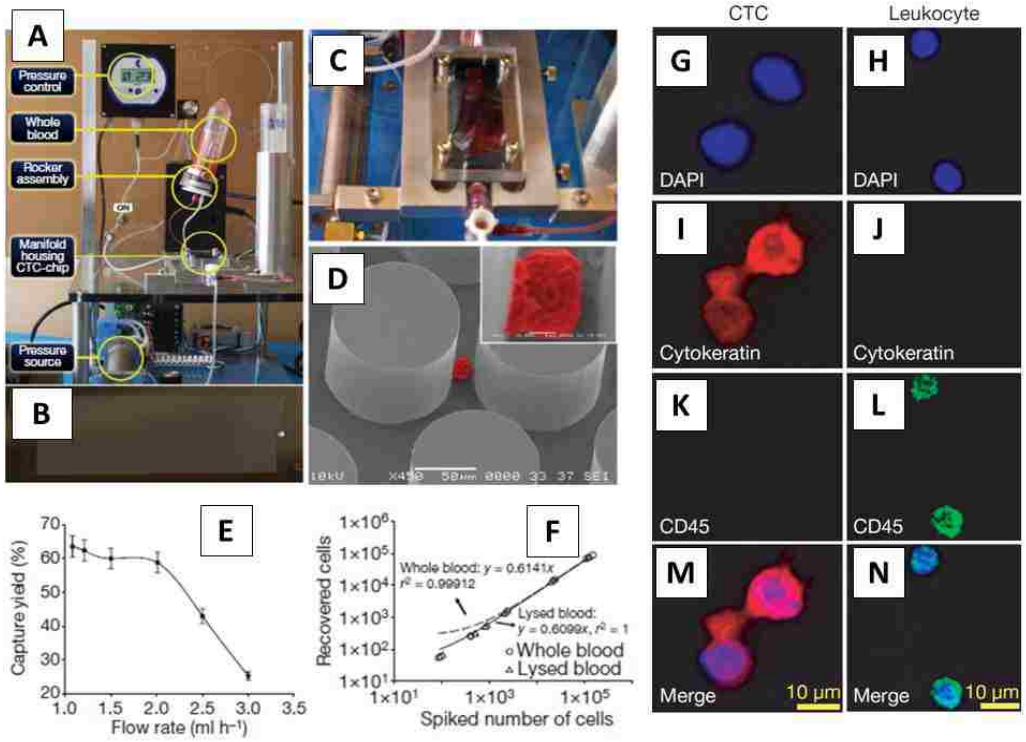

Figure 1.5 Isolation of circulating tumor cells (CTCs) from whole blood, performed with a CTC chip. (A) The workstation setup for CTC isolation from whole blood. (B) The CTC chip with microposts etched into the silicon. (C) Micrograph of whole blood flowing through the CTC chip. (D) An image of a captured NCI-H1650 lung cancer cell spiked into blood. The inset shows a high-magnification view of the captured cell. (E) CTC recovery as a function of flow rate. (F) Regression analysis of capture efficiency for various target-cell concentrations in whole-blood samples versus lysed-blood samples. (G-N) High-magnification images of captured CTCs and hematologic cells stained with 4‘,6-diamidino-2-phenylindole (DAPI), cytokeratin, and CD45. Merged images identify CTCs in panels G, I, K and M and hematologic cells in panels H, J, L and N[33]

Using a flow rate of 1 ml/h, 65% of the CTCs were recovered, and 98% of the cells remained viable. The maximum shear stress that cell near the micropost surface experienced was 0.4 dyn cm^{-2} at $\theta = 68°$. Overall, this CTC chip has the ability to identify large numbers (99%, 40% purity) of viable CTCs

without the use of pre-processing steps.[33]

Adams *et al.* introduced a high throughput microsampling unit (HTMSU) that was fabricated from PMMA and capable of isolating intact CTCs from peripheral blood and directly quantifying the CTC following isolation and enrichment.[36] The device, shown in Figure 1.6, consisted of a series of 51 high aspect ratio channels that were linear or sinusoidally configured with a shared set of input/output ports.

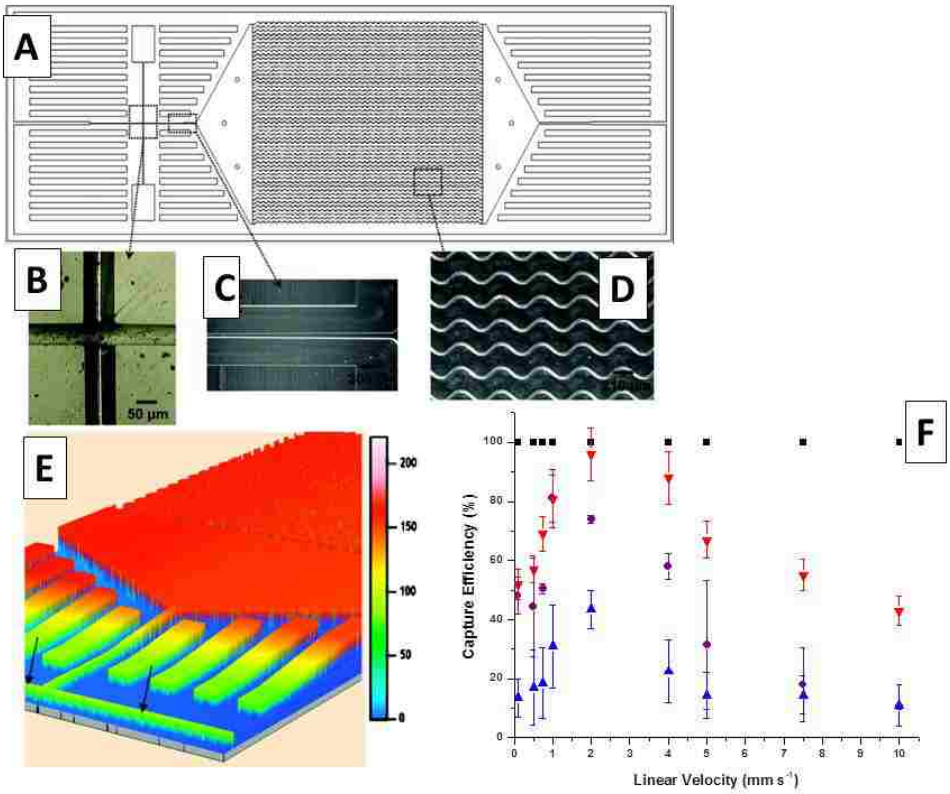

Figure 1.6 Schematic of a microchip-based high-throughput microsampling unit (HTMSU) fabricated in poly (methylmethacrylate) via microreplication for selection of circulating tumor cells (CTCs). (A) An AutoCAD® diagram of the sinusoidally shaped capture channels with bright-field optical micrographs showing (B) the integrated conductivity sensor consisting of cylindrical Pt electrodes with a 75 µm diameter and a 50 µm gap; (C) the single port exit, where the HTMSU's width tapers from 100 µm to 50 µm and the depth tapers from 150 µm to 80 µm over a 2.5 mm region that ends 2.5 mm from the Pt electrodes; (D) the sinusoidal cell-capture channels (5x magnification); (E) three-dimensional projection of the topology of the HTMSU obtained at 2.5 µm resolution via noncontact optical profilometry (arrows, Pt electrode conduits); and (F) the capture efficiency of CTCs in spiked whole-blood samples as a function of the cells' translational velocity. The microchannels were 35 µm wide (red down triangles, sinusoid; purple circles, straight) and 50 µm wide (blue up triangles).[34]

Using the MCF-7 cell line from a metastatic breast cancer patient, capture efficiencies up to 97% were obtained and 1 mL of sample was processed in ~37 min. The captured CTCs were removed from the

capture surface using trypsin and counted individually using conductivity detection.[34]

In 2010, Stott *et al*. introduced a high throughput microfluidic device, the herringbone chip (HB chip), which allowed cells to have adequate contact with antibody-coated surfaces.[32] This device effectively captured CTCs from patients with metastatic prostate cancer. The HB-chip was composed of a 1" x 3" glass slide bonded to a polydimethylsiloxane (PDMS) structure that contained 8 microchannels fabricated with patterned herringbones on their upper surface (Figure 1.6). The internal walls of the device were chemically activated by in-line functionalization and coating with antibodies against EpCAM. The geometric design was based on low Reynolds' numbers (Re). Re is a critical non-dimensional parameter used in microfluidics to characterize the flow stability, which is given by;

$$Re = \rho U d_h / \mu \qquad \text{(Equation 1)}$$

where ρ is the fluid density, U is the fluid velocity, μ the viscosity of the fluid, and dh is the hydraulic diameter of the channel, given by;

$$dh = 4wh/2(w + h) = 2wh/w + h \qquad \text{(Equation 2)}$$

Low Re numbers indicate laminar flow. If the Reynolds number is greater than 2000, the flow would be characterized as turbulent, and therefore would not be conducive for maintaining the viability of CTCs.[34]

This HB-chip was adapted to isolate rare cells from whole blood by varying the ratio of height of the grooves to that of the channel, chevron dimensions and periodicity (Figure 1.6 B). The herringbone grooves were staggered periodically so that each mixing cycle was defined by two sequential regions of ten asymmetrically shifted chevrons. The final dimensions of the device were: overall height of channel (*h*) 50 μm, ratio of the height of the grooves to that of the channel (α) set to 0.8; angle between the herringbones and the axis of the channel (θ) 45°, and principal wave vector q = 2π/100 μm. There was also a branching inlet header that was designed to feed into eight individual channels to promote mechanical integrity and uniform flow distribution across the device. [32] This **"**second generation**"** device offered higher blood volume throughput, and increased CTC capture efficiency and purity. This device also provided imaging benefits because of its transparent walls. It possessed less complex three-

dimensional structures that greatly facilitated scale up device production, thus enabling the initiation of larger-scale clinical studies.

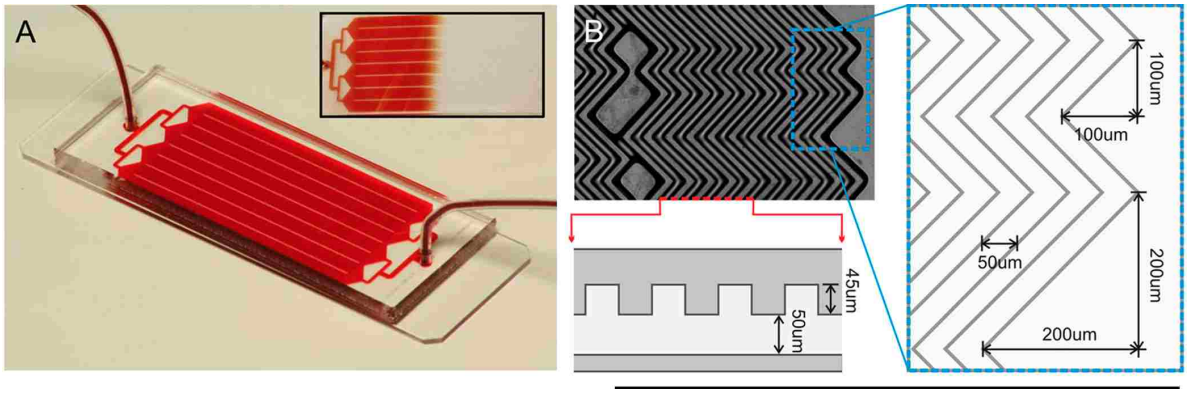

Fig. 1.7. (A) The HB-Chip consists of a microfluidic array of channels with a single inlet and exit. Inset illustrates the uniform blood flow through the device. (B) A micrograph of the grooved surface illustrates the asymmetry and periodicity of the herringbone grooves.[32]

In the initial proof of principle experiments, the HB-chip isolated CTCs from 14 of 15 (93%) patients with metastatic prostate cancer (median 63 CTCs/mL) and allowed for RNA-based detection of the TMPRSS2-ERG fusion transcript, showing a further improvement over the previous generation CTC-Chip reported by Nagrath.[32, 33]

1.9 Conclusions

Evidence has shown that CTCs play a prognostic role in both early and metastatic breast cancer patients.[19, 20] In early breast cancer, the presence of CTCs can allow clinicians to identify those patients at risk for recurrence and therefore may benefit from additional therapy. In both early and metastatic breast cancer patients, CTCs are an easily obtainable option for monitoring treatment efficacy, as they can be collected simply by the drawing of peripheral blood.[19] CTC assessment has been repeatedly shown to be a strong and reliable predictor of outcome in metastatic breast cancer. While the mechanism of CTC generation through release from a primary tumor site is not fully understood, CTCs remain a unique and heterogeneous cell population with established prognostic and predictive value in MBC and more specifically, in defined subtypes of breast disease and may be related to bone biology in particular.[7]

1.10 References

1. Dharmasiri, U.; Balamurugan, S.; Adams, A. A.; Okagbare, P. I.; Obubuafo, A.; Soper, S. A., *Electrophoresis* **2009,** *30* (18), 3289-3300.

2. Yang, S.-Y.; Lien, K.-Y.; Huang, K.-J.; Lei, H.-Y.; Lee, G.-B.,. *Biosensors & Bioelectronics* **2008,** *24* (4), 855-862

3. Lee, W.-C.; Lien, K.-Y.; Lee, G.-B.; Lei, H.-Y., *Diagn. Microbio. Infect. Dis.* **2008,** *60*, 19.

4. Kagan, M.; EP, D.; HA, F., Tumor Markers: Physiology, Pathobiology, Technology and Clinical Applications. **2002**, 5.

5. Kagan, M.; Howard, D.; Bendele, T.; Mayes, J.; Silvia, J.; Repollet, M.; Doyle, J.; Allard, J.; Tu, N.; Bui, T.; Russell, T.; Rao, C.; Hermann, M.; Rutner, H.; Terstappen, L., *Journal of Clinical Ligand Assay* **2002,** *25* (1), 104-110.

6. Moll, R.; Lowe, A.; Laufer, J.; Franke, W. W.,. *American Journal of Pathology* **1992,** *140* (2), 427-447.

7. Swaby, R. F.; Cristofanilli, M., *Bmc Medicine* **2011,** *9*.

8. Ashworth, T., *Aust. Med. J.* **1869,** *14*.

9. Brooks, S.; Lomax-Browne, H.; Carter, T.; Kinch, C.; Hal, D., *Acta Histochem.* **2010,** *112*.

10. Pachmann, U. A.; Hekimian, K.; Carl, S.; Ruediger, N.; Rabenstein, C.; Pachmann, K., *WebmedCentral Cancer* **2011,** *2*.

11. Fidler, I. J., *Journal of the National Cancer Institute* **1970,** *45* (4), 773-&.

12. Mocellin, S.; Keilholz, U.; Rossi, C. R.; Nitti, D., *Trends in Molecular Medicine* **2006,** *12* (3), 130-139.

13. Blood, C.; Zetter, B., *Biochim. Biophys. Acta. Rev. Cancer* **1990,** *1032*.

14. Hendrix, M.; Seftor, E.; Kirschmann, D.; Quaranta, V.; Seftor, R., *Cancer Biol & Therapy* **2003,** *2*, 6.

15. Perl, A. K.; Wilgenbus, P.; Dahl, U.; Semb, H.; Christofori, G., *Nature* **1998,** *392* (6672), 190-193.

16. Price, J.T.; Bonovich, M.T.; Kohn, E.C., *Cri. Rev. in Biochem. and Mol. Bio.* **1997,** *32* (3), 175-253.

17. Friedl, P.; Wolf, K., *Cancer Research* **2008,** *68* (18), 7247-7249.

18. Yu, M.; Stott, S.; Toner, M; Maheswaran, S.; Haber, D. A., *Journal of Cell Biology 2011,* 192 (3), 373-382.

19. Graves, H.; Czerniecki, B. J., *Pathology research international* **2011,** *2011*, 621090.

20. Husemann, Y.; Geigl, J. B.; Schubert, F.; Musiani, P.; Meyer, M.; Burghart, E.; Forni, G.; Eils, R.; Fehm, T.; Riethmueller, G.; Klein, C. A., *Cancer Cell* **2008,** *13* (1), 58-68.

21. Lu, J.; Fan, T.; Zhao, Q.; Zeng, W.; Zaslavsky, E.; Chen, J. J.; Frohman, M. A.; Golightly, M. G.; Madajewicz, S.; Chen, W.-T., *International Journal of Cancer* **2010,** *126* (3), 669-683.

22. Dawood, S.; Broglio, K.; Valero, V.; Reuben, J.; Handy, B.; Islam, R.; Jackson, S.; Hortobagyi, G. N.; Fritsche, H.; Cristofanilli, M., *Cancer* **2008,** *113* (9), 2422-2430.

23. Sledge, G. W., Jr., *Clinical Cancer Research* **2006,** *12* (21), 6321-6322.

24. Attard, G.; de Bono, J. S., *Current Opinion in Genetics & Development* **2011,** *21* (1), 50-58.

25. Dharmasiri, U. Louisiana State University, Baton Rouge, 2010.

26. Tibbe, A. G. J.; Miller, M. C.; Terstappen, L. W. M. M., *Cytometry Part A* **2007,** *71A* (3), 154-162.

27. Alison, A. L.; Keeny, M., *J. Oncol.* **2010**.

28. Nannmark, U.; Johansson, B.; Bagge, U., **1991,** (9).

29. Balic, M.; Dandachi, N.; Hofmann, G.; Samonigg, H.; Loibner, H., Cytom. B Clin. Cytom. **2005,** *6*

30. Cristofanilli, M.; Hayes, D. F.; Budd, G. T.; Ellis, M. J.; Stopeck, A.; Reuben, J. M.; Doyle, G. V.; Matera, J.; Allard, W. J.; Miller, M. C.; Fritsche, H. A.; Hortobagyi, G. N.; Terstappen, L., *Journal of Clinical Oncology* **2005,** *23* (7), 1420-1430.

31. Riethdorf, S.; Fritsche, H.; Mueller, V.; Rau, T.; Schindibeck, C.; Rack, B.; Janni, W.; Coith, C.; Beck, K.; Jaenicke, F.; Jackson, S.; Gornet, T.; Cristofanilli, M.; Pantel, K., *Clinical Cancer Research* **2007,** *13* (3), 920-928.

32. Stott, S. L.; Hsu, C.-H.; Tsukrov, D. I.; Yu, M.; Miyamoto, D. T.; Waltman, B. A.; Rothenberg, S. M.; Shah, A. M.; Smas, M. E.; Korir, G. K.; Floyd, F. P., Jr.; Gilman, A. J.; Lord, J. B.; Winokur, D.; Springer, S.; Irimia, D.; Nagrath, S.; Sequist, L. V.; Lee, R. J.; Isselbacher, K. J.; Maheswaran, S.; Haber, D. A.; Toner, M., *Proc. of the Natl Acad.of Sci. of the USA* **2010,** *107* (43), 18392-18397.

33. Nagrath, S.; Sequist, L. V.; Maheswaran, S.; Bell, D. W.; Irimia, D.; Ulkus, L.; Smith, M. R.; Kwak, E. L.; Digumarthy, S.; Muzikansky, A.; Ryan, P.; Balis, U. J.; Tompkins, R. G.; Haber, D. A.; Toner, M., *Nature* **2007,** *450* (7173), 1235-U10.

34. Adams, A. A.; Okagbare, P. I.; Feng, J.; Hupert, M. L.; Patterson, D.; Goettert, J.; McCarley, R. L.; Nikitopoulos, D.; Murphy, M. C.; Soper, S. A.,. *Journal of the American Chemical Society* **2008,** *130* (27), 8633-8641.

CHAPTER 2. CAPTURE AND ENUMERATION OF BREAST CANCER CTCs WITH LOW EpCAM EXPRESION LEVELS USING anti-EpCAM ANTIBODIES IMMOBILIZED TO A MICROFLUIDIC POLYMERIC DEVICE

2.1 Introduction

Breast cancer is the most frequently diagnosed non-cutaneous cancer and remains the second leading cause of cancer deaths among women in the United States.[1] It is estimated that out of 8 women at least 1 will develop an invasive breast cancer at some point during her lifetime. Conventionally, contrast enhanced magnetic resonance imaging has been used to evaluate women who have been diagnosed with breast cancer.[1] Unfortunately, despite optimal and systemic adjuvant treatment, 30-40% of patients diagnosed with curable breast cancer will face fatality. These facts demand the need for novel approaches for breast cancer diagnosis, prognosis and treatment, which could potentially be accomplished using breast cancer CTC analysis.

This project will investigate the utility of a microfluidic device that possesses a 51 channel capture bed that has been covalently decorated with anti-EpCAM antibodies directed against breast cancer CTCs.[2] In particular, we were interested in selecting CTCs that possess low expression levels of EpCAM because many clinical samples contain CTCs that are heterogeneous including the amount of EpCAM they express. CTCs that have low expression levels of EpCAM can be difficult to collect because the low EpCAM expression level can induce poor adhesion to the surfaces decorated with anti-EpCAM antibodies. To evaluate the ability to select CTCs with low EpCAM expression levels, the MDA-MB-231 breast cancer cell line was used in this study because it possesses a low EpCAM expression level; 1.7 x 10^3 binding sites per cell.[3] This expression level is so low, that MDA-MB-231 cells are often characterized as EpCAM negative.[3] The aforementioned microfluidic device has been used to obtain high recoveries (>97%) of breast cancer CTCs with high EpCAM expression levels (MCF-7).[2] The MCF-7 breast cancer cell line has an EpCAM expression level of 222.1 x10^3 binding sites per cell.[3]

EpCAM, the epithelial cell adhesion molecule, is a glycoprotein encoded from the GA-733-2 gene located on chromosome 2.[4] EpCAM expression is restricted to and broadly expressed by cells of epithelial

origin.[5] The overexpression of EpCAM has been reported in carcinomas and is associated with poor prognosis. Expression of EpCAM in various carcinomas has led to research to evaluate the use of anti-EpCAM antibodies as possible a treatment for patients diagnosed with metastatic cancer.[4] Osta *et al.* demonstrated that EpCAM is highly overexpressed in primary and metastatic breast cancer. EpCAM has also been determined to be a contributor to the proliferation, migration, and invasion of breast cancer cells.[5] The specific noncovalent interactions between a ligand, such as an EpCAM antibody, and a target-specific receptor, EpCAM, is exploited through the use of affinity based selection of CTCs.[6] Positive selection occurs when a target cell is directly captured through the use of a membrane protein that is unique to that cell type and its associated antibody.[7] Cell selection consists of a solid phase in which (a) the recognition element(s) is covalently tethered to the surface and (b) the sample containing the CTCs is moved through a conduit to facilitate the selection process.[7] Other factors that play a role in the efficiency of the interaction between the cell's membrane antigen and surface-bound antibody are: (a) Non-specific interactions; (b) target cell-recognition element adhesion strength; (c) conduit architecture; (d) recognition element immobilization chemistry; and (e) ligand surface density.[7]

The cell/surface antibody adhesion force (F_A) is critical to affinity-based cell selection that uses surface-immobilized recognition elements and flow processing because large F_A of the target cell to the surface enhance the recovery.[7] The F_A between the cell and antibody-decorated surface must be greater than the shear force (F_S) generated by the solution flow to prevent target cell loss.

F_A can be calculated from the bond strength between a single antigen-antibody complex (f_c), the cell-contact area with the recognition surface (A_c), and the number of limiting receptor sites poised within the contact area of the cell to the surface (C_s). The number of receptor sites is either determined by the load level of antibodies to the surface or the expression level of the antigen on the CTC. In most cases, C_s is set by the antibody surface density, however, in the case of CTCs that have low expression levels of EpCAM, C_s is determined by the surface concentration of the antigens. F_A is calculated from Equation 1,[2]

$$F_A = f_c \, x \, A_c \, x \, C_s \, . \qquad \text{(Equation 1)}$$

Once the cell adheres to the capture surface, the contact area can be calculated from Equation 2, if the cell is assumed to be a non-deformable object. [2]

$$A_c = \pi \{r_p \sin[\cos -1(r_p - h' + h)/r_p]\}^2 \qquad \text{(Equation 2)}$$

where r_p is the cell radius and h and h′ represent the characteristic cell-separation distances from the surface upon binding. For MCF-7, which has an EpCAM expression level of 5.1×10^5 per cell, the adhesion strength was calculated to be 0.26 dynes assuming a non-deformable object.[2] In the case of MDA-MB-231 cells, where the EpCAM expression level is 1.7×10^3 per cell, F_A is now equal to 0.0013 dynes. Therefore, a larger contact area (A_c) would be required to for the MDA-MB-231 cells to provide sufficient adhesion strength to minimize loss during flow processing (see below).

In the event that the shear force, F_S, generated by the flow is equal to or greater than F_A, the cell can be removed from the surface. The velocity-dependent F_S can be determined from Stoke's law, Equation 3,[2]

$$F_S = 6 \pi \eta r_p \nu_c \qquad \text{(Equation 3)}$$

where r_p is the cell radius, η is the solution viscosity, and ν_c is the critical linear velocity that can induce cell detachment.

Wang *et al.* demonstrated the utility of a three-dimensionally (3D) nanostructured substrate coated with anti-EpCAM antibodies that has the ability to isolate CTCs from whole blood.[8] A silicon-nanopillar (SiNP) array was used to allow for enhanced interactions between the SiNP substrates and nano-scale components of the CTC surface, which ultimately resulted in improved cell-capture affinity in comparison to unstructured substrates.

The 3D nanostructured cell capture substrates were prepared by fabricating densely packed nanopillars with diameters of 100-200 nm on silicon wafers using a wet chemical etching method.[8] SiNPs were created with lengths ranging from 1-20 μm by applying different etching times. The N-hydroxysuccinimide (NHS)/maeimide chemistry was used to introduce streptavidin to the surface of the

SiNP. Following this biotinylated anti-EpCAM antibody was added to the streptavidin coated substrates to create an anti-EpCAM antibody immobilized substrate. An MCF-7 cell suspension was introduced onto a 10 μm long SiNP surface and incubated for an hour. In parallel, a flat Si substrate modified with anti-EpCAM antibodies was also examined as a control. The substrate immobilized cells were visualized using fluorescence microscopy. It was determined that the SiNP substrates could capture up to ten times more cells than the flat Si substrates. Flat Si substrates only achieved capture yields of 4-14% as opposed to 45-65% on SiNP substrates. It was concluded that the 3D nanostructures are possibly responsible for the enhanced cell capture yields. This conclusion was drawn from the fact that enhanced topographic interactions between the 3D nanostructured substrates and extracellular extensions existed, in addition to anti-EpCAM antibody/EpCAM biological recognition.[8]

This chapter will explore the generation of unique surface architectures for the high efficiency recovery of low expression level EpCAM expressing cells, such as MDA-MB-231 breast cancer cells. In particular, we will look at the percent recovery of CTCs obtained using the high throughput microfluidic device described previously with different surface processing conditions to enhance the recoveries.[2] The effects of anti-EpCAM antibody concentration on the percentage of breast cancer CTCs recovered will also be investigated.

2.2 Materials and Methods

PMMA substrates and cover plates (0.5 mm thickness) were purchased from Good Fellow (Berwyn, PA). Polyimide-coated fused silica capillaries were purchased from Polymicro Technologies (Phoenix, AZ). Chemicals used for the PMMA surface cleaning and modification included reagent grade isopropyl alcohol, 1-ethyl-3-[3-dimethylaminopropyl] carbodimide hydrochloride (EDC), N-hydroxysuccinimide (NHS), fetal bovine serum and 2-(4-morpholino)-ethane sulfonic acid (MES) and these were purchased from Sigma-Aldrich (St. Louis, MO). Monoclonal anti-EpCAM antibody was obtained from R & D Systems (Minneapolis, MN). The MDA-MB-231 cells were cultured at the Louisiana State University Agricultural Science laboratory. Phosphate buffered saline (PBS) was purchased from American Type Culture Collection (ATCC, Manassas, VA). All solutions were prepared in 18 MΩ water. PKH67, a

fluorescein derivative, which contained a lipophilic membrane linker for cell staining, was purchased from Sigma-Aldrich.[3,4]

2.2.1 Cell Suspensions

MDA-MB-231 cells were cultured to 80% confluence in Dulbecco's Modified Eagle's Medium supplemented with high glucose containing 1.5 g L-1 sodium bicarbonate ($NaHCO_3$), 15 mM HEPES buffer, and 10% fetal bovine serum. A 0.25% trypsin solution was prepared in 150 mM PBS and used to harvest the MDA-MB-231 cells from the culturing plate.

MDA-MB-231 cells were stained with PKH67 for microscopic visualization experiments using fluorescence. A modified protocol for cell staining was employed in which the dye concentration was increased twofold. This increase resulted in more evenly distributed fluorescent labels over the cell's periphery. Cell counts for seeding experiments into PBS buffer were determined by counting three aliquots of cells in succession using a hemacytometer.

2.2.2 Fabrication of HTMSU

The HTMSU was hot embossed into PMMA substrates via micro-replication from a metal mold master.[9] Fabrication of the HTMSU used protocols that have been previously reported.[2 9] The HTMSU consisted of a series of 51 high-aspect ratio curvilinear channels that collectively formed the cell selection bed. Each channel was 150 μm (depth) x 30 μm (width) and shared common inlet/outlet ports. Curvilinear-shaped capture channels were used to improve the capture efficiency as described previously. Curvilinear channels do not possess the cell-free marginal zone that occurs in straight channels. The use of curvilinear channels stops the cell radial distribution from being affected by changes in cell translational velocity.[9] Centrifugal forces acting on the cells and the cross stream velocity component due to the reversal of the direction of curvature, causes the cells to migrate to the outside of the curved channels.[2] This resulted in an increase in the antibody/antigen encounter rate as the cells moved through the capture beds at high-linear velocities, which resulted in high recoveries of the CTCs.[3] The channel width of the cell capture bed (30 μm) was similar to the average target cell diameter. This channel width was chosen to increase the probability of cell-antigen interactions with the target cells. The large channel

depth (150 µm) was selected to decrease the pressure drop in high-volume flow rate operation and also to increase the sample processing throughput.[3] In Figure 2, the entry (a) was connected to a T intersection labeled (e). All of the channels were rectangular in shape with dimensions of 50 µm x 100 µm, width and depth, respectively.[2, 9] The chips were washed in micro 90 critical cleaning solution and 2-propanol. They were ultrasonicated for 25 min. The channels were observed under a microscope to ensure that they were not filled with debris. They were then dried overnight in an oven at 70°C.

2.2.3 Antibody Immobilization to the HTMSU

The properly cleaned HTMSU substrates and cover plates were exposed through a mask to UV radiation, which resulted in regio-specific carboxylation only in the exposed areas of the PMMA.[9]

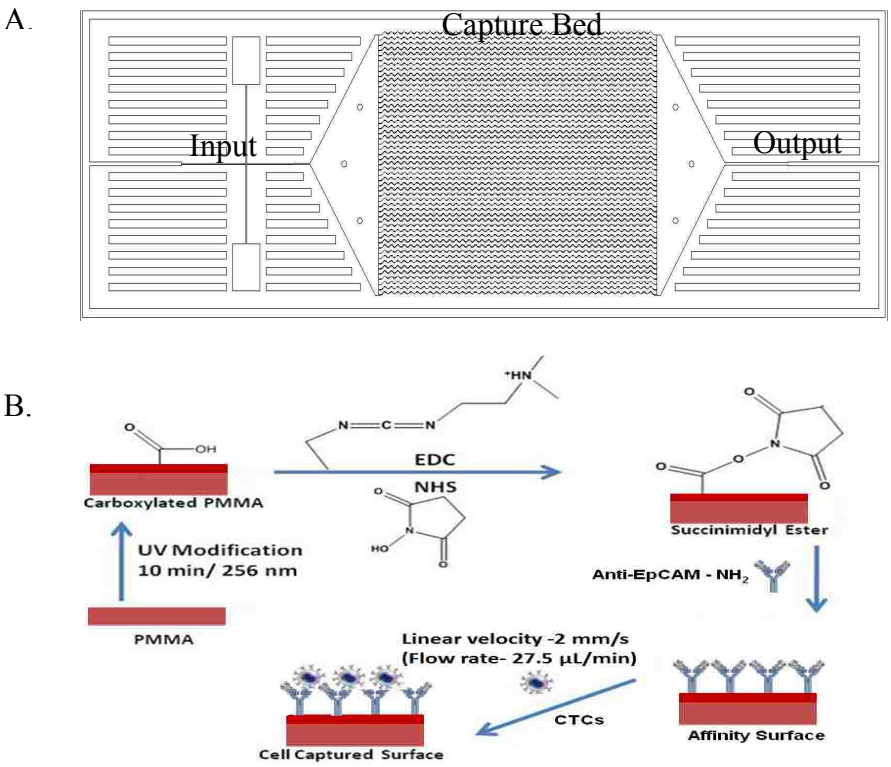

Figure 2.1 (A) Diagram of the HTMSU made via micro-replication into PMMA from a metal mold master. The capture bed consisted of curvilinear channels that were 30 µm wide and 150 µm deep (51 channels). (B) Antibody immobilization scheme for the selection of MDA-MB-231 cells. Also shown is the chemistry used for the immobilization of the EpCAM antibodies to the PMMA surface. The first step involved the UV-irradiation (20.76 mW/ cm^2) of PMMA and in this case, the irradiation was carried out on just the capture bed so that positive cell selection occurred only in this region.[2]

UV radiation was exposed through a mask for 5, 10, 15 or 20 min at 20 mW cm^{-2} to generate an activated surface that included a carboxylic acid scaffold.[3,4] The EpCAM antibody immobilization scheme is shown in Figure 2.1. The UV-modified HTMSU device was infused with a solution that contained 6 mg/mL EDC, 40 mg/m NHS in 150 mM MES (pH = 6). The device containing the EDC/NHS reaction mixture was then incubated for 15 min at room temperature in order to produce a succinimidyl ester intermediate. Following incubation, the EDC/NHS solution was removed by flushing nuclease-free water through the device.

Antibody immobilization to the HTMSU device's microchannel walls was initialized by introducing a 0.25, 0.5, 1.0 or 2.0 μg/μL aliquot of monoclonal anti-EpCAM antibody solution contained in 150mM MES (pH = 6) into the microfluidic device. The antibody infused device was then allowed to react overnight in darkness and moisture. To facilitate EpCAM antibody immobilization exclusively, the device was then rinsed with PBS solution (pH = 7.4) to remove any non-specifically bound EpCAM antibodies.[9]

2.2.4 MDA-MB-231 Cell Capture Using the HTMSU

The HTMSU was connected to a PHD2000 syringe pump (Harvard Apparatus, Holliston, MA using a luer lock syringe (Hamilton, Reno, NV) that was modified with a luer-to-capillary adapter (Inovaquartz, Phoenix, AZ).[9] This was then attached to the capillary that was sealed to the input port of the HTMSU. A pre-capture rinse was performed with 0.2 mL of 150 mM PBS at 50 mm s^{-1} linear velocity to maintain isotonic conditions. Then, 1mL of the cell suspension was introduced at a flow rate of 27.5 μL/min to produce the desired linear velocity in each microchannel that comprised the capture bed. Next, a post-capture rinse was performed with 0.2 mL of 150 mM PBS (pH = 7.4) at 50 mm s^{-1} to remove any non-specifically adsorbed cells. In order to optically visualize the captured cells, the PMMA devices were fixed onto a programmable motorized stage of an Axiovert 200M (Carl Zeiss, Thornwood, NY) microscope and video images were collected during each experiment at 30 frames per second using a monochrome CCD (JAI CV252, San Jose, CA). A Xe arc lamp was used to excite the fluorescent dyes incorporated into the cells membrane.[4] Cells were quantified in one channel using a hemacytometer. The

number of cells counted in one channel was multiplied by 51 to aid in the determination of percent recoveries.

2.2.5 IR Measurements of UV-Modified PMMA

IR spectra of pristine and UV modified PMMA (5, 10, 15, 20 min) was obtained using a Bruker Tensor 27 FT-IR. The standard sample cell was a Pike Miracle single-bounce attenuated total reflectance (ATR) cell equipped with a ZnSe single crystal. ZeSe absorbs strongly below 650cm^{-1}. The IR beam penetrated approximately 60 μm into the surface of the PMMA. Background spectra were collected before each measurement.

2.3 Results and Discussion

The analysis of breast cancer CTCs is challenging and often results in low cell recoveries and poor reproducibility.[7] The low recoveries are related to the rarity of CTCs in human blood (~10 cells/mL of whole blood). CTC isolation techniques, such as immunomagnetic bead purification, (*i.e.* CellSearch) isolate small numbers of CTCs (4 ±2) per ml in lung; 11 ±12 in breast; 10 ±33 in prostate; and 1 ±2 in both colorectal and pancreatic cancers with very low purity (0.01–0.1%), and low yield (20–60% of patients).[10]

Microsystem platforms allow one to manipulate small numbers of cells without loss of sample.[7] Eliminating cell loss is difficult when using macro-scale techniques, such as flow cytometry, which requires a starting population of more than 100,000 cells.[6] One challenge in utilizing low-abundance cell selection assays using microsystems is sampling; the ability to generate a high statistical probability of selecting the low-abundance cells requires large input volumes (>1 mL) to be processed, and most microsystems cannot handle large-volume inputs in reasonable times (*i.e.*, they have poor throughput).[7]

This creates the necessity for a novel microfluidic design that will accommodate the appropriate sample volume.[7] The capture of breast cancer CTCs using the HTMSU has been previously reported by Adams *et al.*[2] The MCF-7 cell line was used as a model for CTC selection and enumeration via and HTMS, which has an EpCAM expression level of 222.1 X 10^3 per cell.[2] Using the MCF-7 cell line, recoveries of 97% were achieved using this microfluidic device.[2]

The work reported herein will show that CTCs exhibiting low EpCAM expression levels can be recovered with high efficiency using similar methods as reported by Adams *et al.* and Dharmasiri *et al*, but with special surface designs/chemistry imparted to the capture bed.[2 9] The device used by Andre *et al.* has the ability to improve the recovery low expression EpCAM cells because it possesses design rules and integration methods capable of changing the surface chemistry without sacrificing its current operational metrics.[2] The system employs efficient high-aspect ratio capture beds. The 51 channels in this capture bed are covalently decorated with EpCAM antibodies through an EDC-NHS reaction. The low EpCAM expressing MDA-MB-231 cell line was utilized for selection of these CTCs to evaluate methods to improve the positive selection of these types of cells. Specifically, we will investigate UV modification time, which not only generates functional groups for antibody attachment, but also can generate nanotextured surfaces. The antibody concentration used for the attachment reaction will also be investigated. Finally, surface characterization techniques will be undertaken as well.

2.3.1 Percent Recovery of CTCs as a Function of UV Modification Time

It has been determined that surface carboxylic acid groups are formed when PMMA surfaces are exposed to UV irradiation and the resulting surface carboxylic acids allow for further functionalization of PMMA-based microfluidic devices.[11]

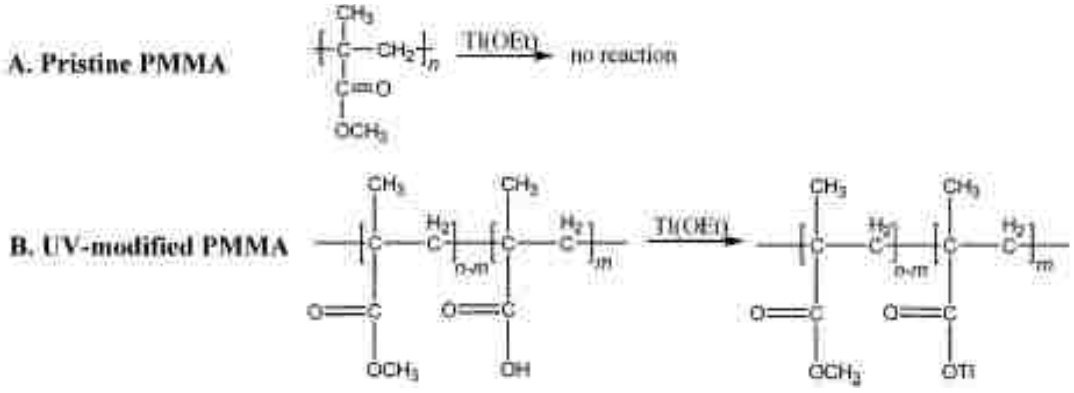

Figure 2.2 (A) Pristine PMMA reacted with Tl(OEt) yields no reaction. (B) UV-modified PMMA reacts with Tl(OEt) to yield Tl labeled PMMA.

In addition, the UV exposure induces photoablation that also creates nanotextured surfaces. This concept was further supported by Batich *et al*., who utilized element specific labeling of UV activated

PMMA surfaces.[12] As outlined in Figure 2.2, Tl (oEt) specifically reacts with carboxylic acid groups, but not ester groups, and therefore the amount of Tl coupled to the polymer surfaces will reveal the number of accessible carboxylic acid groups formed on the polymer.[12]

UV modification was used to generate a carboxylate scaffold on the walls of the HTMSU channels and then, a EDC-NHS reaction was used to generate reactive intermediates that possess the ability to covalently attach to anti-EpCAM antibodies.[2] The capture of MDA-MB-231 cells occurs through the affinity of anti-EpCAM antibodies immobilized to the PMMA surface for the EpCAM antigen that is expressed on the surface of breast cancer CTCs, namely MDA-MB-231 cells. Herein, the effects of varied UV modification times on the percentage of CTCs recovered by the HTMSU device was explored.

The capture bed of the PMMA substrate was exposed to UV irradiation (21.8 mW/cm^2) for 5, 10, 15 and 20 minutes. After thermal fusion bonding of the cover plate and substrate to enclose the fluidic network and the application of the EDC-NHS reaction to immobilize the anti-EpCAM antibodies to the HTMSU channel walls, fluorescently labeled MDA-MB-231 cells were infused into the device at a rate of 27.5 µL/min. Cells were visualized using a Zeiss Axiovert 200M microscope. Table 2.1 shows this data.

Table 2.1 Percent recovery of MDA-MB-231 CTCs versus UV-modification time.

UV Modification Time (min)	Mean Recovery (%) n=3
5	58 ±2
10	82 ±2
15	82 ±3
20	78 ±6

UV modification times as low as 5 min were sufficient for the efficient capture of this low expression level breast cancer CTCs. However, the highest recovery was generated for a 10 min UV modification time, where the recovery was found to be 82 ±2%.

2.3.2 IR Spectra of Pristine and UV Modified PMMA

To obtain evidence of the generation of carboxylic acids as a result of UV modification, IR spectra were collected of pristine PMMA and PMMA that had been exposed to UV irradiation for 5, 10, 15 and 20 minutes. Figure 2.3 shows the IR spectra for pristine PMMA and a 10 min UV modification time,

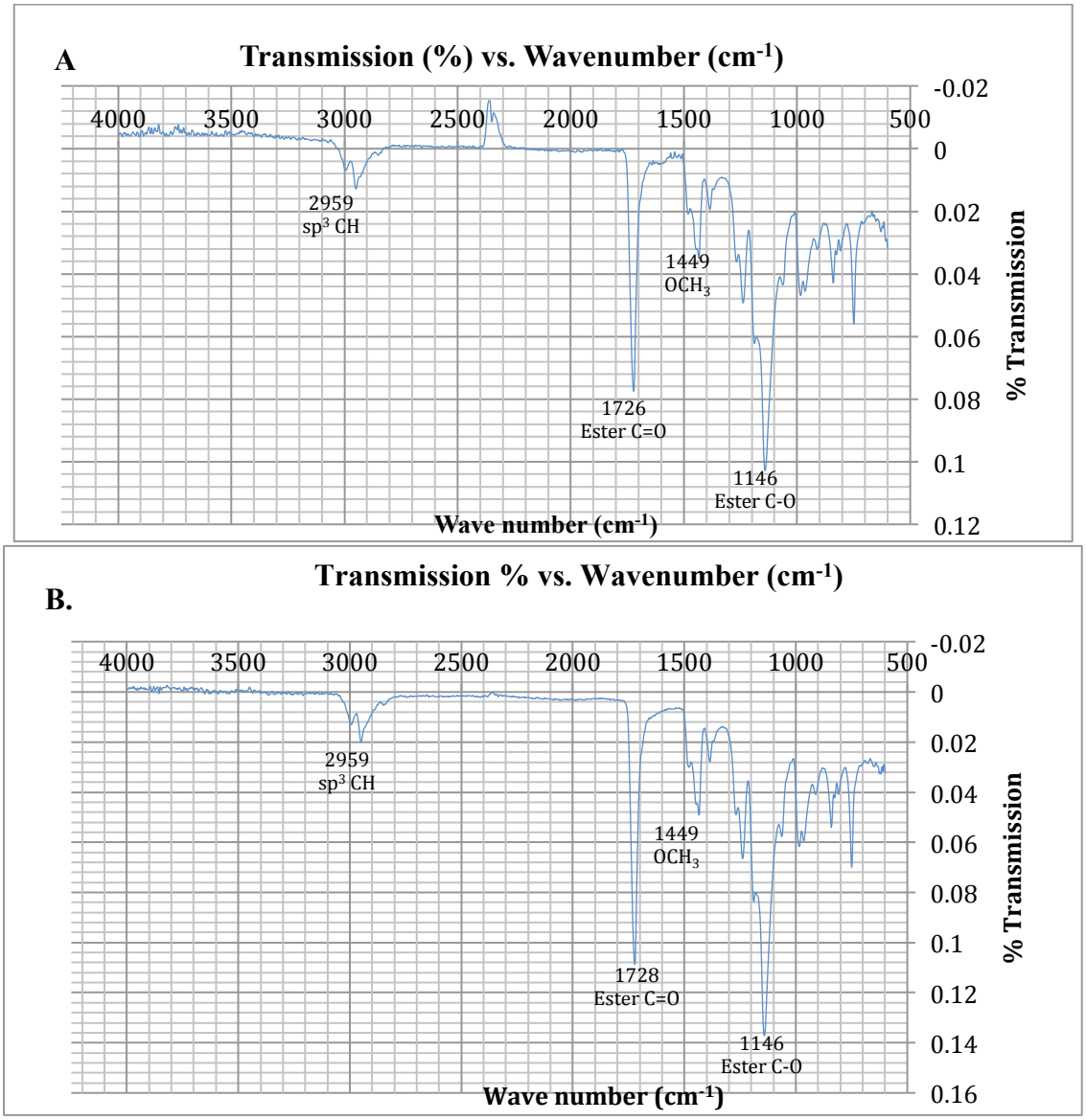

Figure 2.3 (A) IR spectrum of pristine PMMA. (B) IR spectrum of PMMA that was UV modified (20.8 MW/cm^2) for 10 min.

which was shown to be the optimal modification time in Section 2.3.1. These spectra were obtained in order to visually observe the chemical changes that occurred during UV modification. The FT-IR spectrum of pristine PMMA in Figure 2.3a displays the details of functional groups that are present in PMMA. The sharp intense peak at 1726 cm^{-1} appeared due to the presence of an ester carbonyl group stretching vibration.[13] The broader peak seen at 1449 cm^{-1} is due to the C-0 (ester bond) stretching vibration.[13] The broad peak seen around 2959 cm^{-1} is due to an alkane (C-H) stretching vibration.

As the PMMA was UV irradiated beginning with its pristine state to 20 min of exposure, the intensity of the ester group peaks decreased. Although there were differences observed in the intensities of the ester group peaks, these differences were minimal and unfortunately, did not conclusively provide evidence of the generation of carboxylic acids groups on the PMMA surface due to UV modification. The IR beam of the Bruker Tensor FT-IR penetrates ~60 μm into the bulk PMMA. However, UV modification has been shown to penetrate only 6 - 8 μm into the PMMA.[14] Due to the high penetration depth of the IR beam, the ATR-IR spectra are dominated by the bulk material and not surface material and as such, the surface changes are masked. A better approach may be to use the chemistry delineated in Figure 2.2.

2.3.3 Percent Recovery as a Function of EpCAM concentration

Further investigation of the ability of anti-EpCAM antibodies to select low expressing breast cancer CTCs was explored by varying the concentration of the anti-EpCAM antibody used for the reaction. Successful capture of the CTCs using small concentrations of anti-EpCAM antibodies (*i.e.* 0.25 μg/μL) could afford the ability to use less anti-EpCAM antibody material and reduce the cost of producing the device as well.

Using the same protocol and optimal UV modification time of 10 min, EpCAM antibody concentrations of 0.25, 0.5, 1.0 and 2.0 μg/μL EpCAM were allowed to react with the succinimidyl ester formed by the EDC-NHS reaction.

Table 2.2 Percent recovery of CTCs as a function of antiEpCAM antibody concentration

antiEpCAM Antibody Concentration (μg/μL)	Mean Recovery (%) n=3
0.25	71 ±2
0.5	82 ±1
1.0	82 ±2
2.0	80 ±3

In Table 2.2, it was observed that when using an anti-EpCAM antibody concentration of 0.25 μg/μL, a recovery of 71 ±2% was obtained. A maximum percent recovery of 82 ±1 % was observed at concentrations of 0.5 and 1 μg/μL of the antibody.

The percent recoveries obtained, indicated that an anti-EpCAM concentration of 0.25 μg/μL does not provide as many immobilized antibodies for cell capture as 0.5 and 1.0 μg/μL concentrations. The recovery of 82% at concentrations of 0.5 and 1.0 μg/μL could indicate that the channels become saturated with immobilized antibodies at this point and therefore, the recovery does not vary. When an even higher anti-EpCAM antibody concentration of 2 μg/μL was used, the recovery slightly decreased to 80 ±3%.

2.3.4 Plasma Oxidation vs. UV Modification

Plasma oxidation is another method for decorating the walls of the microfluidic channels with carboxylic acid groups to allow for anti-EpCAM antibody attachment. Surface modification of the PMMA occurs when the plasma impinges on the PMMA surface with high energy gas molecules that can result in a variety of reactions on the surface of the PMMA.[14] Herein, we explored the effects of using plasma oxidation as the surface modification method for antibody immobilization instead of UV modification. The goal was to determine if a plasma oxidized HTMSU would yield higher recoveries to those obtained using a UV modified HTMSU. Plasma oxidation was done for 2 min. The CTC percent recoveries are shown in Table 2.3. Brown *et al.* conducted experiments to determine the extent of reaction and the amount of carboxylic acid groups formed on the surface of plasma treated PMMA.[14] The polymer was modified with N-(3-dimethylaminopropyl)-N'-ethylcarbodiimide (WSC), which binds selectively and quantitatively to carboxylic acid groups. The change in WSC concentration was measured after the removal of PMMA. It was found that after 10 s of plasma exposure, there was an increase in carboxylic acid groups (210 ±70 nmol cm^{-2}).[14] UV modification of PMMA follows a similar pattern.[15] Wei *et al* demonstrated that the surface concentration of carboxylate groups on PMMA surfaces increases consistently with increases in photochemical modification time up to 30 min. The surface coverage of carboxylic acid sites on PMMA surfaces can go as high as 1.68 nmol cm^{-2}.[15]

However, in the case of plasma oxidized surfaces, at longer exposure times, a decrease in carboxylic

acid concentration on the surface was observed.[14] The results shown in Table 2.3 were obtained after 2 min of plasma oxidation treatment.

Table 2.3 CTC Percent recovery obtained via plasma oxidation for 2 min.

Cells Infused Into System	**Cells Captured**	**Percent Recovery**
500	240	48%
500	255	51%
500	255	51%

The percent recoveries obtained were lower than those obtained using UV modification. The lower recoveries observed could have been due to a lower number of carboxylate groups that were available for antibody attachment for the plasma treated surface. It has also been reported that plasma oxidized PMMA shows an increased hardness on the surface. This hardness is due to the formation of a brittle layer that arises from the formation of not only carboxylate groups, but also oxides and anhydrides in the exposed region.[14] The combination of functional groups that are formed as a result of plasma oxidation (carboxylates and oxides) could also be a contributing factor to the lower recoveries obtained in comparison to those of a UV modified HTMSU, which may produce lower levels of non-carboxylic acid groups.

Because increased roughness values have been associated with higher recoveries of CTCs, AFM images of plasma oxidized and UV modified PMMA were obtained.[16] These AFM images were used to quantify the differences in roughness between plasma oxidized and UV modified PMMA. Figure 2.4 displays these images. AFM measurements were obtained for pristine, 30 s plasma oxidized and 10 min UV modified PMMA. The roughness values of these modified PMMA surfaces were determined to be 2.2 ± 0.6 nm, 5.5 ± 0.8 nm and 6.6 ± 0.5 nm, respectively. The UV modified surface had the highest roughness and did yield the highest recovery of CTCs (82%).

A.

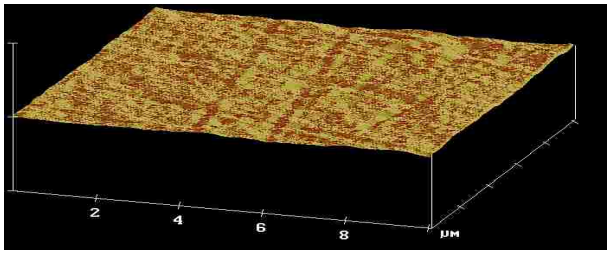

B.

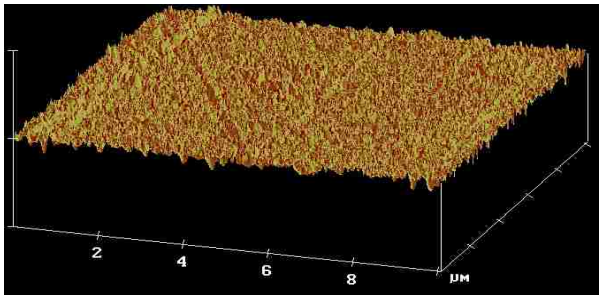

C.

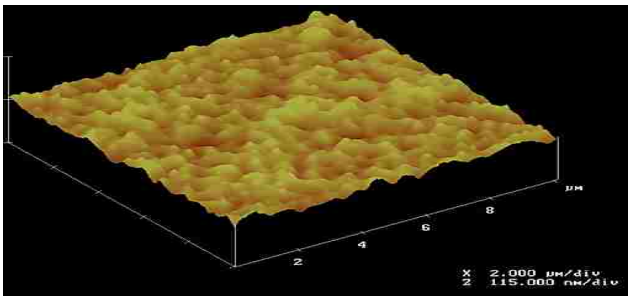

Figure 2.4 AFM images of modified PMMA (A) AFM image of pristine PMMA. (B) AFM image of 30s plasma oxidized PMMA (C) AFM image of 10 min UV modified PMMA.

2.4 Conclusions

Breast cancer CTCs that have low expression levels of EpCAM (MDA-MB-231) can be successfully selected using the HTMSU shown in Figure 2.1, containing channels that have been covalently decorated with anti-EpCAM antibodies. When varying UV modification times of the PMMA (5, 10, 15 and 20 min), a maximum CTC recovery of 82% was achieved when the exposure time exceeded 10 min. The effects of using different concentrations (0.25, 0.5, 1 and 2 µg/µL) of anti-EpCAM antibody were investigated as well. It was found that using anti-EpCAM antibody concentrations as low as 0.25 µg/µL,

71.4% of the cells were recovered. A maximum recovery of 82% was obtained using anti-EpCAM antibody concentrations of 0.5 and 1.0 μg/μL.

When comparing CTC recovery using UV modified microfluidic devices to those that were treated using plasma oxidation, it was determined that the percentage of cells recovered from the latter modification method were lower (51%) compared to the UV modified surfaces. This is most likely due to the fact that plasma oxidation generates hydroxyl and carboxylate groups on the surface of PMMA and the modification chemistry employed was specific for carboxylic acid groups only.[14] In contrast, UV modification exclusively generates carboxylate groups on the surface, therefore allowing for the formation of a greater number of reactive intermediates that will tether to the anti-EpCAM antibodies for CTC selection.

Using UV activation of the appropriate time, sufficient amounts of antibody, we have demonstrated that CTCs typically viewed as EpCAM-negative can be selected from clinical samples. This is attractive, because in most cases, the CTCs selected from a patient represent a heterogeneous population with a large spread in the EpCAM expression level. Therefore, precise CTC numbers can be collected for these patients to better predict patient outcomes from the selected therapy or even guiding therapy. In addition, the higher recovery for even low-expression level CTCs will provide a greater yield to aid in the subsequent molecular profiling of the CTCs from a single patient to help manage his/her particular disease.

2.5 References

1. Graves, H.; Czerniecki, B. J., *Pathology research international* **2011,** *2011*, 621090.

2. Adams, A. A.; Okagbare, P. I.; Feng, J.; Hupert, M. L.; Patterson, D.; Goettert, J.; McCarley, R. L.; Nikitopoulos, D.; Murphy, M. C.; Soper, S. A., *Journal of the American Chemical Society* **2008,** *130* (27), 8633-8641.

3. Prang, N.; Preithner, S.; Brischwein, K.; Goster, P.; Woppel, A.; Muller, J.; Steiger, C.; Peters, M.; Baeuerle, P. A.; da Silva, A. J., *British Journal of Cancer* **2005,** *92* (2), 342-349.

4. Rao, C. G.; Chianese, D.; Doyle, G. V.; Miller, M. C.; Russell, T.; Sanders, R. A.; Terstappen, L., *International Journal of Oncology* **2005,** *27* (1), 49-57.

5. Osta, W. A.; Chen, Y.; Mikhitarian, K.; Mitas, M.; Salem, M.; Hannun, Y. A.; Cole, D. J.; Gillanders, W. K., *Cancer Research* **2004,** *64* (16), 5818-5824.

6. Koo, O. K.; Liu, Y.; Shuaib, S.; Bhattacharya, S.; Ladisch, M. R.; Bashir, R.; Bhunia, A. K., *Anal. Chem.* **2009,** *81* (8), 3094-3101.

7. Dharmasiri, U.; Witek, M. A.; Adams, A. A.; Soper, S. A., In *Annual Review of Analytical Chemistry, Vol 3*, Yeung, E. S.; Zare, R. N., Eds. Annual Reviews: Palo Alto, 2010; Vol. 3, pp 409-431.

8. Wang, S. T.; Wang, H.; Jiao, J.; Chen, K. J.; Owens, G. E.; Kamei, K. I.; Sun, J.; Sherman, D. J.; Behrenbruch, C. P.; Wu, H.; Tseng, H. R., *Angewandte Chemie-International Edition* **2009,** *48* (47), 8970-8973.

9. Dharmasiri, U.; Balamurugan, S.; Adams, A. A.; Okagbare, P. I.; Obubuafo, A.; Soper, S. A., *Electrophoresis* **2009,** *30* (18), 3289-3300.

10. Allard, W. J.; Matera, J.; Miller, M. C.; Repollet, M.; Connelly, M. C.; Rao, C.; Tibbe, A. G. J.; Uhr, J. W.; Terstappen, L., *Clinical Cancer Research* **2004,** *10* (20), 6897-6904.

11. Wei, S. Y.; Vaidya, B.; Patel, A. B.; Soper, S. A.; McCarley, R. L., *Journal Of Physical Chemistry B* **2005,** *109* (35), 16988-16996.

12. Batich, C.; Wendt, R., *ACS Symp. Ser* **1981,** *162*, 14.

13. Balamurugan, A.; Kannan, S.; Sellvaraj, V.; Rajeswari, S., *Trends Biomater. Artif. Organs* **2004,** *18*, 5.

14. Brown, L.; Koerner, T.; Horton, J. H.; Oleschuk, R. D., *Lab on a Chip* **2006,** *6* (1), 66-73.

15. Wei, S., Vaidya, A., Patel, Ami B., Soper, Steven A., McCarley, Robin L. **2005,** 109, 16988-16996

16. Wan, Y.; Mahmood, M.; Li, N.; Allen, P.; Kim, Y.; Bachoo, R.; Ellington, A.; Igba, S., *Cancer* **2011**.

CHAPTER 3. FUTURE WORK: MOLECULAR PROFILING OF CTCs

3.1 Introduction

Analysis of CTCs, for example in the case of breast cancer, is important because of its utility in patient prognosis and potentially diagnosis as well as monitoring for disease recurrence or determining the effectiveness of treatment. CTCs in the blood have been shown to be an important indicator of the potential for relapse and ultimately metastatic disease.[1] Once the CTCs are selected, a means of determining their gene expression is necessary to decipher the activity of genes involved in the patient's cancer disease. Determining the gene expression profiles of CTCs is important because changes in the phenotype of the CTCs can occur after the original diagnosis.[2] Figure 3.1 outlines the genetic flow of information, which is necessary when defining gene expression. A gene is a region of DNA that controls hereditary characteristics.[3] Genes are expressed as the proteins they encode. It occurs in two steps, transcription, followed by translation. Therefore, disregulation occurring due to uncontrolled cell growth, a common phenomena in cancer, can produce proteins that are disregulated as well.

Resistance to treatment is only determined after the treatment has failed.[2] Molecular profiling, of which gene expression profiling is one type of molecular assay, is one way to make this determination.[2] It can be described as the classification of tissue or other specimens for diagnostic and predictive purposes based on multiple gene expression.[4] This information has the potential to improve the management of a cancer patient's treatment regime.[3] Knowledge of genetic alterations or gene expression perturbations in cancer patients can decrease toxicity by avoiding unnecessary therapy in patients who have an excellent prognosis without requiring the need for chemotherapeutic treatment and in those who are deemed unresponsive to a particular therapy.[5] Breast cancer was the first cancer-related disease that molecular profiling has been approved for clinical use.[2] Molecular profiling differs from standard methodologies because it allows tumors to be defined by the expression pattern or genomic alteration of thousands of genes simultaneously instead of relying on a few pathological features and immunohistochemical markers.[6]

There are a number of different molecular profiling techniques including gene expression profiling. A

A. B.

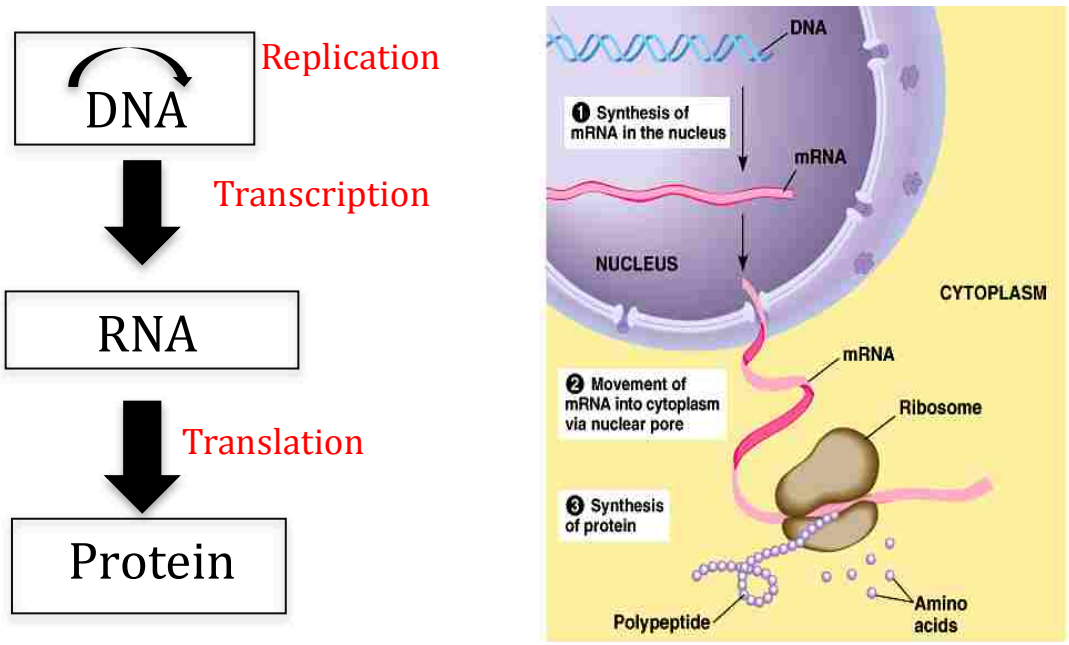

Figure 3.1 (A) The flow of genetic information is unidirectional, from DNA to protein with messenger RNA as an intermediate (B) Genetic Flow of Information: Proposed by Francis Crick in 1958 to describe the flow of information in a cell. [3]

major difficulty encountered when choosing a molecular profiling technique is that many cancers, such as breast cancer, are highly heterogeneous and contain a mixture of benign, cancerous and stromal cells when performing the analysis directly on tumor tissue.[7] Current methodologies such as RT-PCR, gene chips, protein chips, 2D gel electrophoresis and biomolecular mass spectrometry are not designed to handle heterogeneous samples with sufficient reliability.[7] In contrast, high-throughput techniques, such as microarray analysis, provide knowledge of mutations or epigenomic changes in certain genes and prognostic and predictive models on the basis of mRNA and microRNA (miRNA) expression profiles.[8] This high throughput technique is an excellent methodology that can prevent excessive or insufficient treatment of cancer patients, however most of these prognostic models are based on the primary tumor and not the subsequent metastasis that occurs.[8] Metastasis, which can develop years after the occurrence of the primary tumor, can possess great genetic differences from the tissue of the primary tumor.[8] It is therefore anticipated that molecular profiling of metastasis will improve current prognostic models.[8] This can be achieved through molecular characterization of CTCs.[8] The molecular profiling technique that will be the focus of this chapter will be gene expression profiling. One application for gene expression

profiling is the use of microarrays.[9] This technology brings the prospect of defining individual genes or combinations of genes whose expression levels can differentiate between clinically significant subtypes of breast tumors that require different treatment strategies.[5]

3.2 Molecular Classification of Breast Cancer

There are various gene mutations that can be expressed by a particular breast cancer disease of a patient. The identification of these mutations give physicians a better insight into the types of therapy that will be needed and the patient's likelihood for relapse.[10] Biological evidence for the heterogeneity of breast cancer has also been provided through molecular profiling. Heterogeneity essentially means that the response to treatment and the prognosis of two patients with the same stage of breast cancer can be considerably different. [2] The intrinsic subtypes of breast cancer, such as Luminal A, Luminal B, HER2+/ER- have been distinguished by gene expression profiling.[11] Perou *et al.* first identified distinct subtypes of breast cancer using unsupervised hierarchal analysis of gene expression pattern differences identified in 65 breast cancer specimens.[12] The sub-classification of breast cancer tumors into luminal and basal-like types originated from comparing gene expression patterns with those of epithelial cells that are normally found in non-malignant human mammary gland tissues.[11] Perou *et al.* proposed that these four classes could be called basal-like cancers, which mainly corresponded to ER-negative, progesterone-receptor (PR) negative and HER2 negative tumors, luminal-A cancers, which are mostly ER positive, luminal B cancers, which are like luminal-A, but may also express low levels of hormone receptors, and HER-2 positive cancers that show amplification and high expression of ERBB2. Luminal types of tumors have been shown to express high levels of luminal cytokeratins and genetic markers of luminal epithelial cells of normal breast tissue through microarray studies.[11]

In contrast, basal-like breast cancers do not express ER, PR, and ER-related genes and do not overexpress several genes that typify myoepithelial cells of normal breast tissue, luminal cytokeratins, smooth-muscle–specific markers, and certain integrins.[7] In some basal-like cancers, there is high expression of "basal" cytokeratins, such as CK5 and a variety of growth factor receptors, including high levels of epidermal growth factor receptor, c-kit (a tyrosine kinase in breast epithelium), and growth

factors such as hepatocyte growth factor and insulin growth.[7]

3.3 Current Methods of Breast Cancer Gene Expression Profiling: Microarrays

Gene expression microarray analysis has a potential role for predicting relapse.[6] Currently, the majority of scientific analyses conducted focus on the manipulation and interpretation of cDNA arrays that are generated by converting mRNAs that have been isolated from various tissue types into cDNAs. These cDNAs are fixed to a solid substrate and then quantified.[9] The principle of a microarray experiment is that mRNA from a given cell line or tissue is used to create a labeled sample, the target, which is hybridized in parallel to a large number of DNA sequences immobilized on a solid surface in an ordered array.[9] Researchers are then able to compare the expression of cDNAs isolated from different tissue types. From the comparative data gathered, scientists are able to better elucidate the biology of each tissue type.[5] This technology has the ability to detect and quantify tens of thousands of transcript species simultaneously.[9]

There are two main types of microarray systems; complementary DNA (cDNA) and oligonucleotide microarrays (Figure 3.2).[9] Included in the cDNA system is a probe, which is the arrayed material. The probes that are generated are PCR products from cDNA libraries or gene specific primers (oligonucleotide). They are printed onto glass slides or nylon membranes as spots at defined locations. These spots can range from 100-300 μm in size and are spaced equal distance apart. Arrays of more than 30,000 cDNAs can fit onto arrays the size of a conventional microscope slide. In the case of oligonucleotide arrays, short 20-25mers are synthesized *in situ* and printed onto glass slides. The oligonucleotide method is advantageous because the sequence information alone can be used to generate the DNA to be arrayed.[9] Some disadvantages are encountered because the oligonucleotide method is expensive and the use of short oligonucleotides result in less specific hybridization and reduced sensitivity.[9] Microarray experimental data consists of a long list of measurements of spot intensities and intensity ratios. These measurements are generated by comparing two samples pairwise or by comparing several samples to a common control.

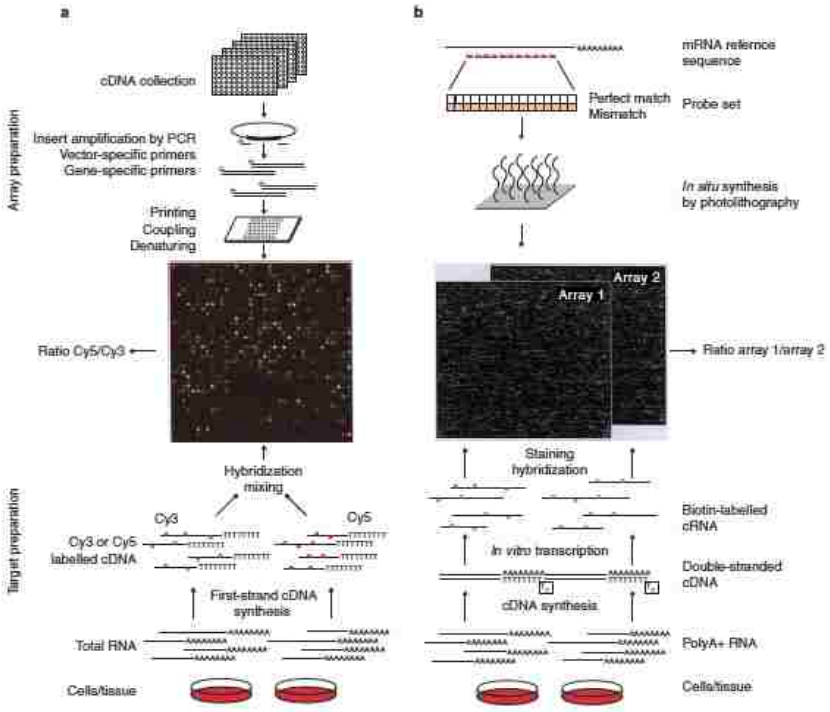

Figure 3.2 Schematic overview of probe array and target preparation for spotted cDNA microarrays and high-density oligonucleotide microarrays. a, cDNA microarrays. b, High-density oligonucleotide microarrays[9]

Following this, the challenge is to sieve through large amounts of data to find results that are significant and meaningful. It has also been discovered that significant variability issues can occur and replication is required to develop a high degree of confidence in the data. Often, subsets of results have to be verified through alternative techniques such as northern hybridization, RNase protection or PCR with RT-PCR.

Overall, microarray technology is capable of differentiating between different subtypes of breast cancer.[9] The biochemistry of microarrays has been proven to be highly useful in developing a complete understanding of the molecular differences in breast cancer samples.[3]

3.4 Future Work Proposal

Evidence presented in Chapter 2 has already shown that breast cancer CTCs that have low expression levels of EpCAM can be successfully captured using a microfluidic device that has been covalently decorated with anti-EpCAM antibodies. This is particularly important for breast cancer, because there are different breast cancer sub-types of various levels of EpCAM expression. For example, claudin-low cells

such as MDA-MB-231, have low EpCAM expression levels and as such, typical positive selection systems due to possess the capability to select these cells. With the discoveries emanating from this

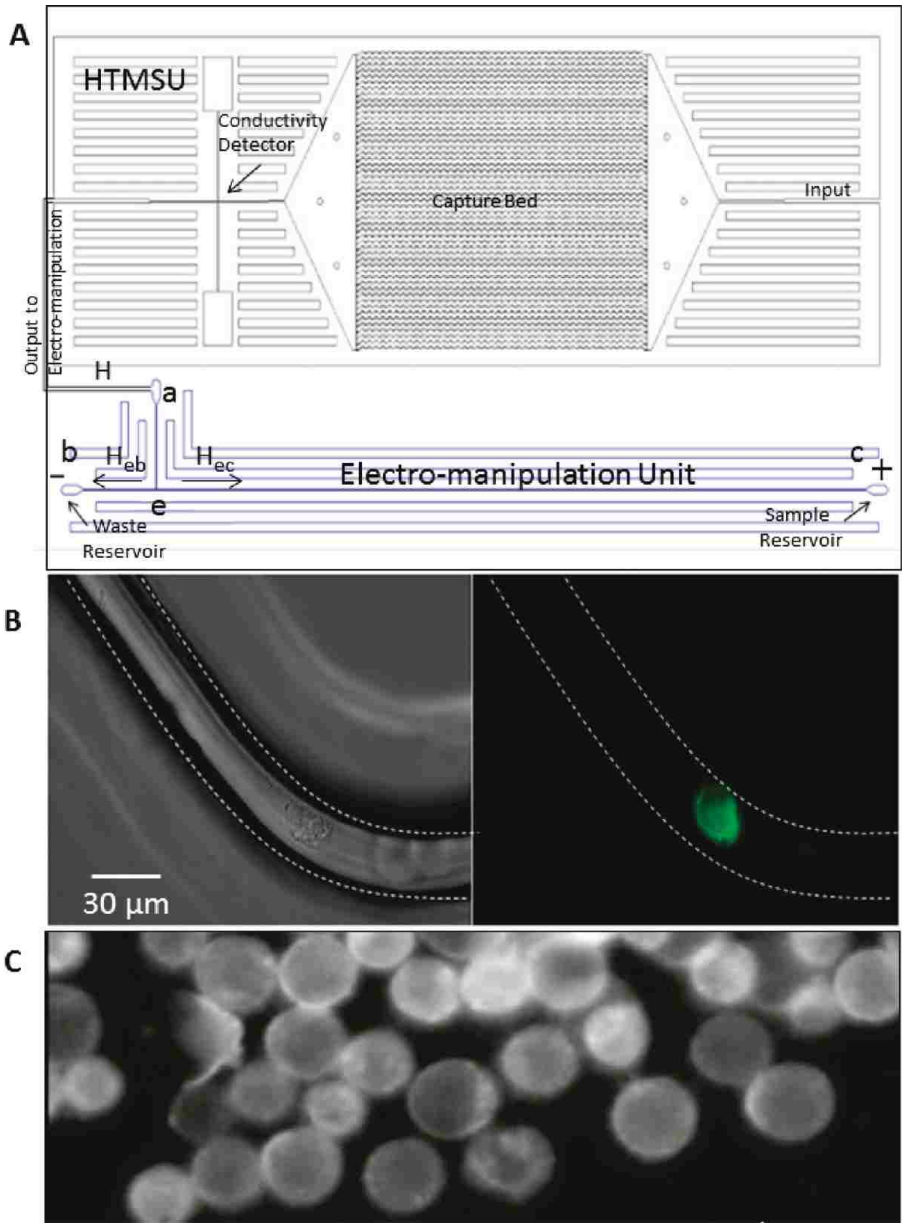

Figure 3.3 Diagrams showing the microfluidic system, which included the HTMSU and the electromanipulation unit. (A) The capture bed consisted of a series of 51 curvilinear channels (30 µm wide and 150 µm deep). The electromanipulation unit contained 80 µm wide, 100 µm deep, and 5 cm long linear channels. Conductometrically enumerated CTCs were introduced into the electromanipulation unit at port a, which served as the entrance port. Port a was connected to a "T" junction labeled e. Exit b served as the sample waste reservoir, while reservoir c was the CTC receiving reservoir (anodic reservoir). (B) Brightfield (left) and fluorescence (right) micrographs (40_) of selected SW620 CTCs using the HTMSU. (C) The selected SW620 CTCs were enriched into reservoir c due to their intrinsic electrophoretic mobility and the applied electric field. The total volume of the receiving reservoir was 2 µL.[13]

work, the use of UV activation and sufficient amount of anti-EpCAM antibodies can generate surfaces that can recover these type of cells with excellent recovery.

The analysis of captured breast cancer CTCs can be taken a step further through molecular profiling. Dharmasiri *et al.* used a similar concept for the capture, enumeration, electrokinetic manipulation and molecular profiling of colorectal CTCs.[13] This study employed a microfluidic electrokinetic manipulation unit interfaced to a fluidic chip to select SW620 and HT29 cells (Figure 3.3).

The microfluidic device was previously described by Adams *et al*. [14] The electro-manipulation unit contained one entry, through reservoir a and two exits, via reservoirs b and c. Reservoir a was connected to a "T" intersection that is labeled e in Figure 3.3. All of the channels were rectangular and had dimensions of 80 μm x 100 μm, width and depth, respectively. Pt wires of 125 μm were used as external electrodes in the b and c reservoirs of the electromanipulation unit.[14] SW620 and HT29 CTCs were captured specifically based on the recognition abilities of anti-EpCAM antibodies that were covalently immobilized to the walls of the HTMSU selection bed.[12] The curvilinear channels of the HTMSU ensured that a high number of cell/wall interactions occurred to improve the recovery.[15] Observation of the selected cells was done using fluorescence and brightfield microscopy. The captured cells were released using 0.25% trypsin, which enzymatically digested the extracellular domain of EpCAM and/or anti-EpCAM antibodies.[13] The average release time was ~16 min. The selected and released cells were then enumerated using conductivity detection.[13] Once released, the CTCs were collected and subjected to a mutation detection assay to look for point mutations in the genomic DNA of the selected CTCs; in this case, Kras mutations were analyzed. This unit used hydrodynamic flow and an electric field to direct CTCs released from the selection surface into a reservoir to allow molecular analysis of low numbers of CTCs.[15] In this study, *KRAS* mutations in the CRC cell lines SW620 and HT29 were used as a model. *KRAS* mutations are indicative of very poor response to panitumumab and cetuximab therapies in colorectal cancers. [15] A PCR coupled to a ligase detection reaction (LDR) assay was conducted on codon 12 of the *KRAS* oncogene of the CTCs. Successful PCRs on 10 CTCs selected from the HTMSU were

confirmed by positive and negative control experiments. The resulting PCR/LDR products were analyzed using capillary gel electrophoresis (Figure 3.4). [13]

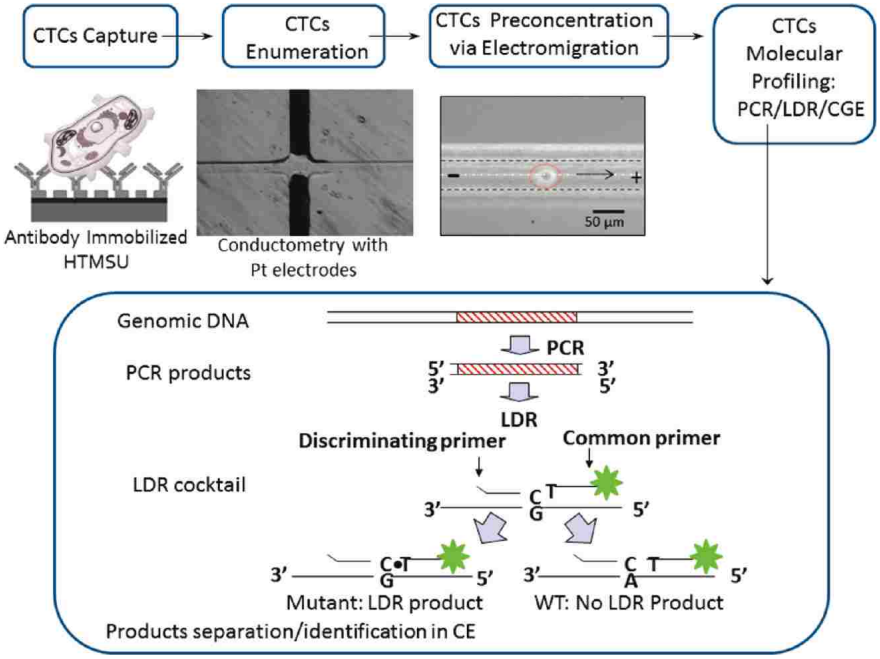

Figure 3.4 Overview for the Cell Selection, Enumeration, Electrokinetic Enrichment, and Molecular Profiling Strategy Adopted for the Analysis of Low-Abundance CTCs Resident in Peripheral Blood[13]

This work explored the idea that immunoaffinity-based selection of CTCS combined with genotyping of the selected CTCs for the presence and absence of certain mutations can give valuable information that will help physicians to determine which treatment regime should be used for a particular colorectal cancer patient.[13] Dharmasiri *et al.* were able to demonstrate the ability to recover CTCs with 96 ± 4% efficiency from whole blood and ~100% electrokinetic enrichment of the selected CTCs.[13] Ten CTCs isolated from whole blood were successfully genotyped.[13]

Given the success of Dharmasiri *et al.*, herein a method is proposed to obtain molecular profiles, of breast cancer CTCs that have been selected using a HTSMU. The abnormal activation of HER1 and HER2 has been linked to various types of breast cancer progression. It has also been reported that there are frequent and significant changes in their expression status between primary tumor and CTCs. [10] Obtaining a molecular profile of these genes from captured breast cancer CTCS using microarray analysis

may provide better insight into the diseases profile shift and ultimately lead to better selection of therapy for individual patients. [10]

3.5 Materials and Methods

PMMA substrates and cover plates (0.5 mm thickness) will be purchased from Good Fellow (Berwyn, PA). Polyimide-coated fused silica capillaries will be purchased from Polymicro Technologies (Phoenix, AZ). Chemicals used for the PMMA surface cleaning and modification will include reagent grade isopropyl alcohol, 1-ethyl-3-[3-dimethylaminopropyl] carbodimide hydrochloride (EDC), N-hydroxysuccinimide (NHS), fetal bovine serum and 2-(4-morpholino)-ethane sulfonic acid (MES) and these will be purchased from Sigma-Aldrich (St. Louis, MO). Monoclonal anti-EpCAM antibody will be obtained from R & D Systems (Minneapolis, MN). The MDA-MB-231 cells will be cultured at the Louisiana State University Agricultural Science laboratory. Phosphate buffered saline (PBS) will be purchased from American Type Culture Collection (ATCC, Manassas, VA). All solutions will be prepared in 18 MΩ water. PKH67, a fluorescein derivative, which contains a lipophilic membrane linker for cell staining, will be purchased from Sigma-Aldrich.[3,4]

3.5.1 MDA-MB-231 Cell Suspensions

MDA-MB-31 cells will be cultured to 80% confluence in Dulbecco‘s Modified Eagle‘s Medium supplemented with high glucose containing 1.5 g L^{-1} sodium bicarbonate ($NaHCO_3$), 15 mM HEPES buffer, and 10% fetal bovine serum.[15] A 0.25% trypsin solution will be prepared in 150 mM PBS and used to harvest the MDA-MB-31 cells from the culturing plate.

MDA-MB-231 cells will be stained with PKH67 for microscopic visualization experiments using fluorescence. A modified protocol for cell staining will be utilized whereby the dye concentration will be increased two-fold resulting in more evenly distributed fluorescent labels over the cell‘s periphery. Cell counts for seeding experiments into whole blood will be determined by counting three aliquots of cells in succession using a hemocytometer.[15]

3.5.2 Fabrication of HTMSU

The microfluidic device will be fabricated using the same methods previously reported by Adams *et. al*.[14] Briefly, The HTMSU (Figure 3.3 A) will be hot embossed into PMMA substrates via micro-replication from a metal mold master. Fabrication of the HTMSU will follow steps previously reported.[14, 16] The HTMSU will consist of a series of 51 high-aspect ratio curvilinear channels that in concert formed the cell selection bed. Each channel will have 150 um (depth) x 30 um (width) and shared common inlet/outlet ports.[14]

3.5.3 Antibody Immobilization to HTMSU

A UV-modified HTMSU device will be infused with a solution that contains 6 mg/mL EDC, 40 mg/m NHS in 150 mM MES (pH=6) and will be incubated for 15 min at room temperature in order to generate a succinimidyl ester intermediate. Following incubation, the EDC/NHS solution will be removed by flushing nuclease-free water through the device. Then, a 0.5 μg/μL aliquot of monoclonal anti-EpCAM antibody solution will be dissolved in 50 mM PBS (pH = 7.4) and will be injected into the HTMSU and allowed to react overnight. The device will then be rinsed with a PBS solution (pH = 7.4) to remove any non-specifically bound anti-EpCAM antibodies.[15]

3.5.4 MDA-MB-231 Cell Capture Using the HTMSU and Release

The HTMSU will be connected to a pump using a luer lock syringe (Hamilton, Reno, NV) equipped with a luer-to-capillary adapter (Inovaquartz, Phoenix, AZ). This will then be attached to a capillary that is sealed to the input port of the HTMSU. A pre-capture rinse will be performed with 0.2 mL of 150 mM PBS at 50 mm s^{-1} linear velocity to maintain isotonic conditions.[15] Then, the appropriate volume of a cell suspension will be introduced at the necessary volumetric flow rate to produce the desired linear velocity in each microchannel comprising the selection bed. Next, a post-capture rinse will be performed with 0.2 mL of 150 mM PBS (pH = 7.4) at 50 mm s^{-1} to remove any non-specifically adsorbed cells. In order to optically visualize the selected cells, the PMMA devices will be fixed onto a programmable motorized stage of an Axiovert 200M (Carl Zeiss, Thornwood, NY) microscope and video images will be collected during each experiment at 30 frames per second using a monochrome CCD (JAI CV252, San Jose, CA).[15]

A Xe arc lamp will be used to excite the fluorescent dyes incorporated into the cells‘ membrane. Following a post-capture rinse, a 0.25% trypsin solution in 0.2 mM Tris/19.2 mM glycine buffer (pH = 8.3) will be infused at 27.5 μL min^{-1} volumetric flow rate into the HTMSU.[15]

3.5.5 RNA Isolation

For gene expression studies following the selection of CTCs using the HTMSU, CTCs will be lysed by adding 100 μL of Trizol reagent (Invitrogen, Carlsbad, CA).[17] For all CTC samples, a CTC depleted blood fraction will be saved by withdrawing 100 μL of blood that will be recovered after CTCs are selected. This fraction will then be placed into a tube that will contain 900 μL of Trizol reagent. RNA from all samples will be isolated using Trizol reagent based on the manufacturer's instructions, DNase I treated and Trizol repurified.[17]

3.5.6 Target Preparation, Microarray Hybridization and Microarray Data Analysis

10 ng of total RNA from the CTC enriched and CTC depleted fractions will be used to prepare biotinylated hybridization targets with Affymetrix's eukaryotic small sample target labeling assay.[17] This protocol is designed to reproducibly amplify 10 to 100 ng of total RNA and is based on the principal of performing two cycles of double-stranded cDNA synthesis and *in vitro* transcription reactions using T7 RNA polymerase.[17] Biotinylated target crane will then be hybridized to an Affymetrix Focus array based on manufacturer's instructions. Gene expression data will be obtained using Affymetrix Microarray Analysis Suite.[17]

3.6 Expected Results and Significance

The anti-EpCAM antibodies will be covalently bonded to the channel walls. This dynamic interaction between anti-EpCAM antibodies and the microchannel walls is necessary for the recovery of the breast cancer CTCs.[15] When the breast cancer CTCs are infused into the system, they will be selectively immobilized. The selected CTCs will be observed and enumerated using brightfield microscopy. The cells will then be released from the capture bed via methods that will have minimal impact on the integrity and viability of the cell.[15]

Following their release, the RNA will be extracted from the CTCs for gene expression analysis

through the use of microarrays. This proposed method will offer the ability to obtain expression profiles for HER1 and HER2 expressed in breast cancer CTCs. It is expected that by using a microarray based test, that multiple, distinct predictions, that include prognosis, ER and HER2 status and sensitivity to various treatment approaches will be generated from a single assay.[10] Ultimately, this method should lead to the successful genotyping of CTCs, that have low EpCAM expression levels from whole blood.

3.7 Clinical Implications

Being that EpCAM overexpression has been linked to poor prognosis and tumor invasiveness, a method that quickly selects and quantifies viable CTCs would prove to be beneficial in a clinical setting. CTC analysis could be used for diagnosis, prognosis and the prediction of treatment methods. The obtainment of CTCs is minimally invasive and would be done simply by drawing the blood of a patient in the clinic. The blood would then be infused into the same HTSMU used in Chapter 2 that consists of a capture bed that has immobilized EpCAM antibodies for the selection of cancer cells that express EpCAM[14] Captured cells would then be released using trypsin.[14] In a clinical setting, it would be unnecessary to visualize the CTCs using a microscope. Clinicians would simply use the conductivity detector that is integrated into the microfluidic device.[14]

Cells would be hydrodynamcally driven through the conductivity sensor using a syringe pump at a controlled flow rate. CTCs will then be detected based on their electrical properties that are unique in comparison to other cells found in whole blood samples. These properties of CTCs make them good candidates for conductivity detection. Based on the simple and low-cost production of these devices using microreplication technologies as well as their automated operation with no sample preprocessing required, the HTMSU would be a perfect fit in a clinic as a diagnostic tool for monitoring CTC levels in a variety of adenoma-based cancers for disease detection, cancer staging or evaluating the effectiveness of therapeutic intervention.[14]

3.8 Thesis Summary

The thesis began with an overview of circulating tumor cells. The term was defined and current methods for their analysis was discussed. Chapter 2 focused on my project, which has been to determine

if breast cancer CTCs with low EpCAM expression levels could be captured using the same methodologies employed by Adams *et al.* and Dharmasiri *et al*.[13, 16] The work described in Chapter 2 confirmed that CTCs with low EpCAM expression levels can indeed be selected and enumerated with high efficiency. It was also determined that the anti-EpCAM antibody concentration can be decreased to select these cells without significantly degrading the CTC recovery.

The thesis was concluded with Chapter 3, which initially described the advantages of taking the analysis of selected CTCs a step further through molecular profiling. Current methods of molecular profiling were included. Finally, future experimental methods for the molecular profiling of selected MDA-MB-31 cells via microarray based analysis were proposed. The overall clinical implications of the HTMSU for capture of CTCs was also discussed.

3.9 References

1. Nagrath, S.; Sequist, L. V.; Maheswaran, S.; Bell, D. W.; Irimia, D.; Ulkus, L.; Smith, M. R.; Kwak, E. L.; Digumarthy, S.; Muzikansky, A.; Ryan, P.; Balis, U. J.; Tompkins, R. G.; Haber, D. A.; Toner, M., *Nature* **2007,** *450* (7173), 1235-U10.

2. Tewes, M.; Aktas, B.; Welt, A.; Mueller, S.; Hauch, S.; Kimmig, R.; Kasimir-Bauer, S., *Breast Cancer Research and Treatment* **2009,** *115* (3), 581-590.

3. Causton, H. C.; Quakenbush, J.; Brazma, A., Blackwell Science Publishing: 2003.

4. Ioannidis, J. P. A., *Oncologist* **2007,** *12* (3), 301-311.

5. Morris, S. R.; Carey, L. A., *Current Opinion in Oncology* **2007,** *19* (6), 547-551.

6. Cleator, S.; Ashworth, A., Molecular profiling of breast cancer: clinical implications. *British Journal of Cancer* **2004,** *90* (6), 1120-1124.

7. Yezhelyev, M. V.; Al-Hajj, A.; Morris, C.; Marcus, A. I.; Liu, T.; Lewis, M.; Cohen, C.; Zrazhevskiy, P.; Simons, J. W.; Rogatko, A.; Nie, S.; Gao, X.; O'Regan, R. M., *Advanced Materials* **2007,** *19* (20), 3146.

8. Sieuwerts, A. M.; Mostert, B.; Bolt-de Vries, J.; Peeters, D.; de Jongh, F. E.; Stouthard, J. M. L.; Dirix, L. Y.; van Dam, P. A.; Van Galen, A.; de Weerd, V.; Kraan, J.; van der Spoel, P.; Ramirez-Moreno, R.; van Deurzen, C. H. M.; Smid, M.; Yu, J. X.; Jiang, J.; Wang, Y.; Gratama, J. W.; Sleijfer, S.; Foekens, J. A.; Martens, J. W. M., *Clinical Cancer Research* **2011,** *17* (11), 3600-3618.

9. Schulze, A.; Downward, J., *Nature Cell Biology* **2001,** *3*, 6.

10. Kao, J.; Salari, K.; Bocanegra, M.; Choi, Y.-L.; Girard, L.; Gandhi, J.; Kwei, K. A.; Hernandez-Boussard, T.; Wang, P.; Gazdar, A. F.; Minna, J. D.; Pollack, J. R., Molecular *Plos One* **2009,** *4* (7).

11. Sotiriou, C.; Pusztai, L., *New England Journal of Medicine* **2009,** *360* (8), 790-800.

12. Perou, C., *Breast* **2011,** *20*, S2-S3.

13. Dharmasiri, U.; Njoroge, S. K.; Witek, M. A.; Adebiyi, M. G.; Kamande, J. W.; Hupert, M. L.; Barany, F.; Soper, S. A., *Anal. Chem.* **2011,** *83* (6), 2301-2309.

14. Adams, A. A.; Okagbare, P. I.; Feng, J.; Hupert, M. L.; Patterson, D.; Goettert, J.; McCarley, R. L.; Nikitopoulos, D.; Murphy, M. C.; Soper, S. A.,. *Journal of the American Chemical Society* **2008,** *130* (27), 8633-8641.

15. Bouche, O.; Beretta, G. D.; Garcia Alfonso, P.; Geissler, M., *Cancer Treatment Reviews* **2010,** *36*, S1-S10.

16. Dharmasiri, U.; Balamurugan, S.; Adams, A. A.; Okagbare, P. I.; Obubuafo, A.; Soper, S. A., *Electrophoresis* **2009,** *30* (18), 3289-3300.

17. Smirnov, D. A.; Zwetzig, D. R.; Foulk, B. W.; Miller, M. C.; Doyle, G. V.; Pienta, K. J.; Meropol, N.; Weiner, L. M.; Cohen, S. J.; Moreno, J. G.; Connelly, M. C.; Terstappen, L. W. M. M.; O'Hara, S. M., *Cancer Research* **2005,** *65*, 4993.

VITA

Brandy Charon Snowden was born in Zachary, Louisiana, to Robert and Anna Snowden. She attended Southern University and Agricultural and Mechanical College in Baton Rouge, Louisiana. She received her Bachelor of Science in Chemistry from Southern University and Agricultural College in 2007. While in undergraduate school, she was involved in various research endeavors such as LS-LAMP, LBRN and Timbuktu. Upon graduation, Brandy worked in the chemical and health research industry at Exxon-Mobil, BASF, Pennington Biomedical Research Center and currently Shintech, LLC. In 2008, she was accepted into the doctoral program in the Department of Chemistry at Louisiana State University. In 2009, she joined the research group of Professor Steven A. Soper. In graduate school she was a member of NOBBCHE and was a Bridge to Doctorate Program Scholar. She also served as the secretary for the Chemistry Graduate Student Council in 2010. Brandy Charon Snowden is a currently a candidate for a Master of Science Degree in analytical chemistry, which will be rewarded to her at December 2011 Commencement at LSU, Baton Rouge.